Investigating the effects of molarity concentration variation over optical band gap for ZnO based thin film

A Thesis Submitted in Partial Fulfilment of the Requirement for the Award of the Degree of

MASTER OF TECHNOLOGY

in VLSI Design

Submitted By
Amit Kumar Bhatt
601662004

Under Supervision of
Dr. Anil Arora
Assistant Professor, ECED

THAPAR INSTITUTE
OF ENGINEERING & TECHNOLOGY
(Deemed to be University)

ELECTRONICS AND COMMUNICATION ENGINEERING DEPARTMENT
THAPAR INSTITUTE OF ENGINEERING & TECHNOLOGY
(A DEEMED TO BE UNIVERSITY), PATIALA, PUNJAB
JUNE, 2018

DECLARATION

I, Amit Kumar Bhatt hereby declare that the work presented in this thesis entitled **" Investigating the effects of molarity concentration variation over optical band gap for ZnO based thin film"** in partial fulfillment of the requirement for the award of degree of Master of Technology (VLSI Design) submitted at Electronics and Communication Engineering Department, Thapar Institute of Engineering & Technology (Deemed to be University), Patiala is an authentic record of work carried out under supervision of **Dr. Anil Arora (Assistant Professor, ECED)** from July 2017 to July 2018. The matter presented in this has not been submitted either in part or full to any other university or institute for the award of any other degree.

Date: 09/08/2018

Amit Kumar Bhatt
6016620004

It is certified that the above statement made by the student is correct to best of my knowledge and belief.

Date: 9/8/18

Dr. Anil Arora
Assistant Professor, ECED
Thapar Institute of Engineering & Technology
(A Deemed To Be University), Patiala, Punjab

ACKNOWLEDGEMENT

First of all, I would like to express my gratitude to **Dr. Anil Arora**, Assistant Professor, Electronics and Communication Engineering Department, Thapar Institute of Engineering & Technology (Deemed to be University), Patiala for his patient guidance and support throughout this report. I am truly very fortunate to have the opportunity to work with him. I found this guidance to be extremely valuable.

I am also thankful to **Dr. Alpana Agarwal**, Head of the Department for providing us adequate environment in carrying the work.

I would also like to thank my friends who have more or less contributed to the preparation of this report. I will be always indebted to them.

Last but not the least, I would like to thank my parents for their years of unyielding love and encourage. They have always wanted the best for me and I admire their determination and sacrifice.

The study has indeed helped me to explore knowledge and I am sure it will help me in my future

DATE: 09/08/2018

PLACE: PATIALA

AMIT KUMAR BHATT

ABSTRACT

Zinc Oxide (ZnO) is a very promising metal oxide semi conductor for applications in many fields like gas sensors, solar cells, and blue and ultraviolet optoelectronics devices. This thesis deals with the effect of molarity concentration on Zinc Oxide (ZnO) and hence gas sensing thin films which are fabricated by a low cost sol-gel spin coating method. The influence of precursor molarity concentration on structural property of ZnO thin films is characterized by X-ray diffraction (XRD) and Ultra Violet visible (UV-visible) spectroscopy. Sol concentration for ZnO thin film is varied from 0.05M to 1M. The study shows that crystallite sizes (grain sizes) vary with variation of sol concentration. The sol with higher concentration results in the increase in the crystallite size. Optimum sol molarity for the sensitivity of NOx gas comes out to be 0.1M. The highest sensitivity is 80% at optimum temperature 300°C. The minimum response time and minimum recovery time for optimum sol molarity which is 0.1M are 23 seconds and 25 seconds at optimum temperature. The energy band gap also gets affected by sol concentration. As molarity of precursor solution increases energy band gap starts to decrease. At higher solution molarity ZnO thin film starts to acquire the properties of the bulk material and hence energy band gap becomes approximate equal at higher solution molarity. By variation in energy band gap conductivity of material affected. It can be stated from energy band results that conductivity of ZnO thin film increases as energy band gap decreases as we move from lower sol concentration to higher sol concentration.

TABLE OF CONTENTS

LIST OF FIGURES

LIST OF TABLES

LIST OF ABBREVIATIONS

MEMS	:	Micro Electro-Mechanical System
Xrd	:	X-ray Diffraction
UV-visible	:	Ultra violet visible
ZnO	:	Zinc Oxide

Chapter 1

Introduction

1.1 Overview of Zinc Oxide

In the present scenario, there are various semiconducting compounds with unique and fascinating properties to explore the possibilities of using them for circuitry fabrications and many other purposes. Zinc Oxide (ZnO) belonging to group II-VI is one of the semiconductors that have been exploited widely for various applications. It is an attractive material used in transparent electrode, surface acoustic wave devices (SAW), solar cell windows, blue and ultraviolet (UV) light emitters, gas sensors and the photovoltaic device.[1-10]. ZnO basically belongs to the category of metal oxide semi conductors. Zinc oxide (ZnO) is a piezoelectric, dielectric, transparent, semiconducting metal oxide. ZnO shows good electrical and optical properties[1, 11]. ZnO contain a Direct Band Gap of 3.3ev at room temperature[12, 13]. ZnO possess large excitation binding energy which is 60mv[14-16]. ZnO has higher melting Point near by 2248 °K due to which it is the hardest Compound of Group II-VI.

ZnO shows very high resistive towards radiation of high energy, that makes it an appropiate compound in the field of space applications. It can be easily etched or remove with the help of all acids and alkalis. Due to this reason, it can be used in the manufacturing of small size devices e.g. transparent electrodes, window materials for displays and solar cells. There are also possible areas of its applications in microelectromechanical systems (MEMS), both in sensors, actuators and in the fabrication of acoustic and electro-optical devices[17-19].

In particular, it is used in gas sensors as gas sensing layer as thin film[20]. An important role has been played by ZnO in the fabrication process of transparent thin film transistors (TFT), by deposition channel layer on a flexible substrate through a process that contain low temperature, realizing transparent TFTs, and achieving extra functions such as photodetectors using Zinc Oxide (ZnO) channel. The deposited Zinc Oxide (ZnO) generally contain a crystalline structure, although the deposition process is carried out even at room temperature[21]. The study of the thin film of Zinc oxide (ZnO) has been continued in recent time as transparent conducting oxide because its good electrical and optical properties in combination with large band gap (>3eV), abundance in nature, the optical transmittance (>80%) in the visible region. Zinc oxide (ZnO) has been targeted as a promising substrate material due to it possess isomorphic structure. ZnO single crystal substrates have numerous advantages due to low conductivity. ZnO possess two different type of crystal lattices. The first is the hexagonal wurtzite lattice which is generally used in the thin film applications. The second structure is the rock salt structure (at high pressure) and this rock salt is a spinal phase.

1.2 Comparison of different semiconductors

Zinc Oxide (ZnO) was prepared in pure form after preparing of silicon (Si) and germanium (Ge). Semiconductors that have wide energy band gap have attracted significant attention because of they are mainly used compounds in the fabrication of optoelectronic devices for generation of short wavelength (λ). ZnO is widely used in field of ultraviolet (UV) portion of the electromagnetic spectrum because of its wide energy band gap[22]. ZnSe, ZnS, GaN, and ZnO have direct energy band gap that shows similar properties. The comparison among these compound semiconductors is shown in Table 1.1. It can be revealed that ZnO that comes under GroupII-GroupVI semiconductor category is very promising compound for many technological applications. These are especially used for optoelectronic field application and for generation of short wavelength (λ) light emitting devices. The high exciton binding energy that is 60 meV of Zinc Oxide gives rise to efficient excitonic emission at room temperature. The Band gap energy of ZnO varies from 3.3 eV up to 4.5 eV with the alloying process. These unparallel nanostructures without ambiguity presents that ZnO is probably the richest family of nanostructures among all materials, both in structure and properties.

Table 1.1 Comparison of different semiconductors

Wide band gap semiconductor	Crystal structure	Lattice parameter (A°)		Band gap (E_g) electron volt	Melting temp.(°K)	Excitation binding energy (MeV)	Dielectric constant	
		a	**b**				ε_0	$\in_r$
ZnO	Wurtzite	3.250	5.206	3.37	2248	60	8.75	3.72
GaN	Wurtzite	31.89	51.85	3.4	1973	21	9.5	5.15
ZnSe	Wurtzite	5.667	-	2.7	1790	20	7.1	5.3
ZnS	Wurtzite	3.84	6.261	3.7	2103	36	9.6	5.7

1.3 Fundamental properties of ZnO

1.3.1 Crystal structure

Zinc oxide has crystallized structure in Three Different Form.

1. Hexagonal wurtzite
2. Cubic zinc blende
3. Cubic rocksalt (rarely observed).

The wurtzite structure is found to be stable crystallite structure and It is most unanimous at ambient conditions. The form of Zinc blende structure can be stabilized by developing ZnO with a cubic lattice structure on substrates. The atoms of zinc and oxygen are tetrahedral in both hexagonal wurtzite and cubic zinc blende structure. The rocksalt structure is similar to the NaCl-type structure and observed at relatively high pressures which is approximate equal to 10 GPa. There is no inversion symmetry between hexagonal

and zinc blende ZnO lattices. This and other lattice symmetry properties are responsible for piezoelectricity of the hexagonal and zinc blende ZnO and in pyroelectricity of hexagonal ZnO. The lattice constants are *a* = 3.25 Å and *c* = 5.2 Å; their ratio between c and a which is *c/a* is approximate equal to 1.60. The ratio is very close to the ideal value for hexagonal cell *c/a* = 1.633. The bonding of ZnO is largely ionic in almost Group II-VI materials. Due to this ionicity, zinc and oxygen planes contain an electric charge. Therefore, to maintain electrical neutrality, these planes reconstruct themselves at the atomic level in most relative materials. This phenomenea of reconstruction of atom does not occur in Zinc Oxide because its surfaces are atomically flat, stable and show no reconstruction[23].

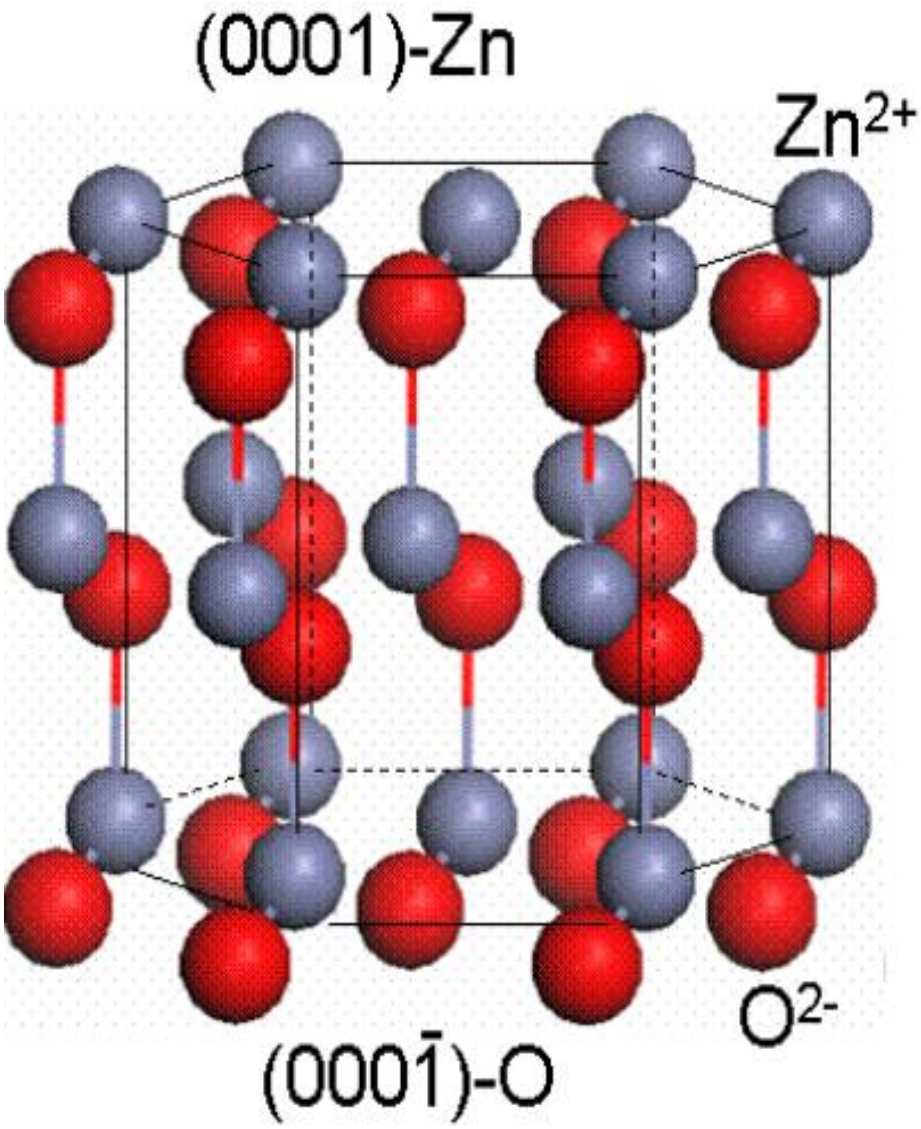

Figure 1.1 ZnO wurtzite crystal structure.

1.3.2 Properties of wurtzite ZnO

In Table 1.2 presents basic physical parameter for ZnO.

Table 1.2 Basic physical properties of ZnO

Property	Value
Lattice parameter at 300 K	
a	3.2495 A°
c	5.2069 A°
c/a	1.602
Density	5.606 g cm^{-3}
Stable phase at 300 K	Wurtzite
Bond length	1977μm
Melting point	1975°C
Thermal conductivity	0.6, 1-1.2
Static dielectric constant	8.656
Refractive index	2.008, 2.029
Energy gap	3.4eV, direct
Exciton binding energy	60MeV
Iconicity	62%
Heat capacity	9.6 cal/mol K
Youngs modulus E(Bulk ZnO)	111.2 $\pm$ 4.7Gpa

1.3.3 Electronic band structure

Electronic band structure is the most important property for any given semiconductor. Properties like Energy band gap and effective electron and hole masses are derived from Electronic band structure. UV-Visible is used as an Experimental method to determine band structure. UV visible is used to determine the electronic core levels in solids. The most important aspect of the band structure of ZnO is that it is a direct energy band gap semi conductor. The energy band gap of ZnO is the difference between the occupied

band and empty bands optical band gap (Eg) that is 3.3eV[24]. These filled states are known the *valence band*, and the energy at the top of the valence band is usually *zero energy* and is known as *valence band edge*. The empty states above the gap are called the *conduction band*. The lowest point in the conduction band is called the *conduction band edge*. The valence band and the conduction band edges of ZnO occur at the same momentum of electron (k)-values is called as *direct band gap semiconductor*[25, 26].

1.3.4 Optical Properties

It depend on both types of effects which are intrinsic effects and extrinsic effects. The phenomena of intrinsic optical transitions happen between the electrons presents in the conduction band and holes which are available in the valence band, including excitonic effects (group velocity of electrons and holes are same) because of the coulomb phenomena, Extrinsic properties depends on dopants or any defects present in semi conductor, that usually generate discrete electronic states in the energy band gap, and therefore influence both optical absorption and emission processes. As it is mentioned above, that ZnO is a direct band gap transparent semiconductor material due to this reason the transparent wavelength (λ) of ZnO films come in range of 0.3μm to 2.5 μm, and depending on the carrier concentration plasma edge lies between 2 and 4 μm. Depending on carrier concentration the shift in energy band gap take place[27-31].

1.3.5 Thermal conductivity

Thermal conductivity is one of the vital property of the semiconductors when the materials are used in the high power application and the high temperature. Kinetic nature is determined by rotation, vibration and electronic degree of freedom. By increasing temperature, Kinetic energy gets affected and causes a decrease in thermal conductivity. Figure 1.2 describe thermal conductivity.

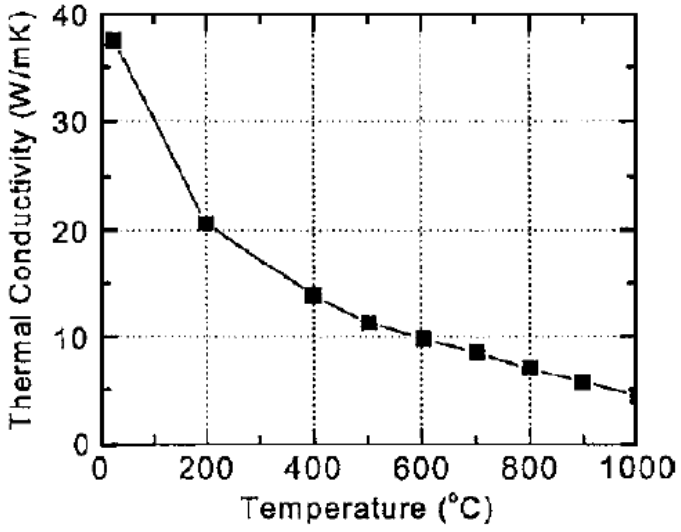

Figure 1.2 Variation in thermal conductivity of fully sintered ZnO heated from room temperature to 1000 °C

1.3.6 Electrical Properties

ZnO is direct and wide band gap semiconductor. It possesses a large exciton binding energy in amount of 60meV, it attracts significant attention regarding optoelectronic and electronic devices. For example, a device developed by a material that has a larger energy band gap may consist a high value of breakdown voltage, lower noise producing and such device can be operated at higher temperatures with high power operation. Electron transport phenomena differs at low value of electric field and high value of electric field in the semiconductor.

At sufficient low electric field, scattering rate does not change such that electron mobility remains constant and the energy distribution of electrons in ZnO remains unaffected. With the increase in value of applied electric field, the energy of electron due to applied electric field is dominant over thermal energy of electron. Due to this electron distribution function varies significantly from its equilibrium value and hence scattering rate is affected and mobility of electron decreases at high electric field[11, 32].

1.4 Thesis organisation

Chapter 1 states to overview of ZnO and its properties.

Chapter 2 describes literature survey regarding deposition techniques of ZnO. It deals with deposition technique what we used further in this thesis.

Chapter 3 presents the methodology and characterization techniques for synthesis of ZnO thin film. This chapter shows procedure of ZnO thin film and description of characterization techniques like Xrd and UV visible.

Chapter 4 describes Results of synthesis of ZnO thin film and further discussion corresponding to results.

Chapter 5 includes Conclusion of what we have performed in this thesis and how this work can be further continued as future scope.

Chapter 2

Literature Survey

2.1 Literature Review

This literature review deals to the techniques used for thin film deposition. Different techniques like Sol gel, CVD (Chemical vapour deposition), Pulse layer deposition (PLD), Magnetron sputtering, chemical precipitation method etc., have been studied for thin film deposition. This literature review gives brief report about the studies of different gas sensing mechanism of ZnO based gas sensor. It also elaborates the different aspects of synthesizing and characterizing techniques used for the ZnO thin film. Table 2.1 illustrates literature review.

Table 2.1 Literature Review

S.No.	Authors	Title	Technique used	Experimental Results
1	L. Znaidi.et.al[33]	Textured ZnO thin films by sol–gel process: Synthesis and characterizations	sol gel	Textured Zinc Oxide thin films have been synthesized using sol gel method by the spin-coating deposition of six coats for each sample.
2	Jiaqi Chen.et.al[10]	Breath Level Acetone Discrimination Through Temperature Modulation of a Hierarchical ZnO Gas Sensor	Chemical vapor deposition (CVD)	A Zinc Oxide gas sensor was fabricated using CVD processes of nanocomb hierarchical shap
3	Ayushi Paliwal.et.al [30]	Dielectric Dispersion of rf Sputter-deposited SnO2, ZnO, WO3 Thin Films	Surface Plasmon Resonance Technique	The thin films of SnO_2, WO_3 and ZnO were deposited by RF sputtering technique on Gold coated BK7 glass. SPR reflectance curves were measured in the Kretschmann geometry.

4	S. Christoulakis.et.al[7]	ZnO transparent thin films for gas sensor applications	Pulse layer deposition (PLD)	AFM and XRD characterization of the films revealed polycrystalline morphology with roughness increasing as the argon partial pressure increases.
5	Jin-Hong Lee.et.al[11]	Electrical and optical properties of ZnO transparent conducting films	sol gel	ZnO thin films were prepared on glass substrates
6	M. Dutta.et.al[27]	Effect of sol concentration on the properties of ZnO thin films prepared	sol gel	The structural, optical and optoelectronic properties of sol gel ZnO thin films have been investigted to be influenced by the concentration of the sol molarity.
7	Mohini Dwivedi.et.al[8]	CO Sensor Using ZnO Thin Film	RF Magnetron sputtering	The ZnO thin film gas sensor is fabricated on Si/SiO2 substrate and used for the sensing of Carbon monooxide gas.
8	A.J. Hashim.et.al[29]	Fabrication and characterization of ZnO thin film using sol–gel method	sol gel	The high quality of Zinc Oxide thin film was fabricated on silicon substrate.
9	Vinod Kumar.et.al[12]	Role of film thickness on the properties of ZnO thin films grown by sol gel method	sol gel	Transparent Zinc Oxide thin films of different thickness were deposited by the sol gel method.
10	Jing Guo.et.al[34]	High-performance gas sensor based on ZnO nanowires functionalized by Au nanoparticles	Hydrothermal method	A high-performance gas sensor based on Au/functionalized.

11	H.Z. Wu.et.al[22]	Low-temperature epitaxy of ZnO "lms on Si(0 0 1) and silica by reactive e-beam evaporation	E-beam evaporation	Optically good-quality of ZnO were achieved on both Si(0 0 1) and silica substrates at low substrate temperature by using reactive e-beam evaporation technique. The optimal growth temperatures are between 200}3003C on Si(0 0 1) and 300}3503C on silica
12	P. F. Carcia. et al[13]	Transparent ZnO thin-film transistor fabricated by rf magnetron sputtering	RF sputtering	Zinc Oxide thin film has been growth on silicon substrate approximate at room temperature with the help of Rf sputtering technique.
13	H. Gong.et.al[9]	Nano-crystalline Cu-doped ZnO thin film gas sensor for CO	sol gel	A nano-crystalline CZO film was prepared by co-sputtering using highly pure ZnO and Cu targets. The CZO film had a columnar structure consisting of nano-crystalline particles of the order of 5 nm in size.
14	BuguoWang. et al[16]	Hydrothermal growth and characterization of indium-doped-conducting ZnO crystals	Hydrothermal	The growth characteristics of crystals of Zinc Oxide under hydrothermal conditions as influenced by impurities, especially by indium ions, have been studied. In3+ in the growth solutions inhibits the growth on [0 0 0 1] but

				permits growth on the m-planes. The crystals grow in plate-like form in the presence of In_3
15	Nitul Kakati.et.al[15]	Thickness dependency of sol gel derived ZnO thin films on gas sensing behaviors	Sol gel	There is increment in roughness of surface. The crystal size increases up to 410nm and starts to decrease from 610nm. The sensitivity of the thin film sensors towards the acetone vapor depends on surface morphology as well as gas concentration.
16	R.C. Pawar.et.al[35]	Surfactant assisted low temperature synthesis of nanocrystalline ZnO and its gas sensing properties	Dip-Coating (sol gel)	It is found that the growth of ZnO nanostructures strongly depends on surfactants.

The above literature review, concludes about different deposition techniques for ZnO deposition. The literature radiates the versatility and lowered cost of fabrication process for the sol gel deposition technique. Hence, for further sample preparation sol gel technique (chemical route) will be followed.

2.2 Sol Gel method

The sol gel method was developed because of the requirement of new synthesis methods in the nuclear industry. A unique method was needed where particle of dust was reduced (compared to the ceramic method) and which needed a low sintering temperature.

The sol gel process may be described as:

"Formation of an oxide network through polycondensation reactions of a molecular precursor in a liquid."

A sol is a stable dispersion of colloidal particles or network of polymers in a solvent. The particles may be in form of amorphous state or crystalline structure. Particles in a gas phase is called as aerosol, and particles in a liquid phase is commonly known as sol.

A gel comprises with a three-dimensional continuous network. It encloses in liquid phase. The colloidal gel contains the network of developed colloidal particles from agglomeration. Generally, particles of the sol may bound by Vanderwaals forces or hydrogen bonds. A gel is also be defined by connecting chains of polymer. In most gel systems, the interactions consist covalent bonding nature and the gel process can not be reverse. Figure 2.1 presents sol processing options.

- The main idea behind sol gel synthesis is dissolve the compound in a liquid solvent, in order to get it back in solid form in controlled manner.
- Sol gel method prohibits the problems of co-precipitation, which may be non-uniform, be a gelation reaction.
- Sol gel method results in small particles sizes, which can be easily sinterable.

Sol gel synthesis may be used to developed materials with a variety of shapes, such as thin films, porous structures, thin fibers, and dense powders.

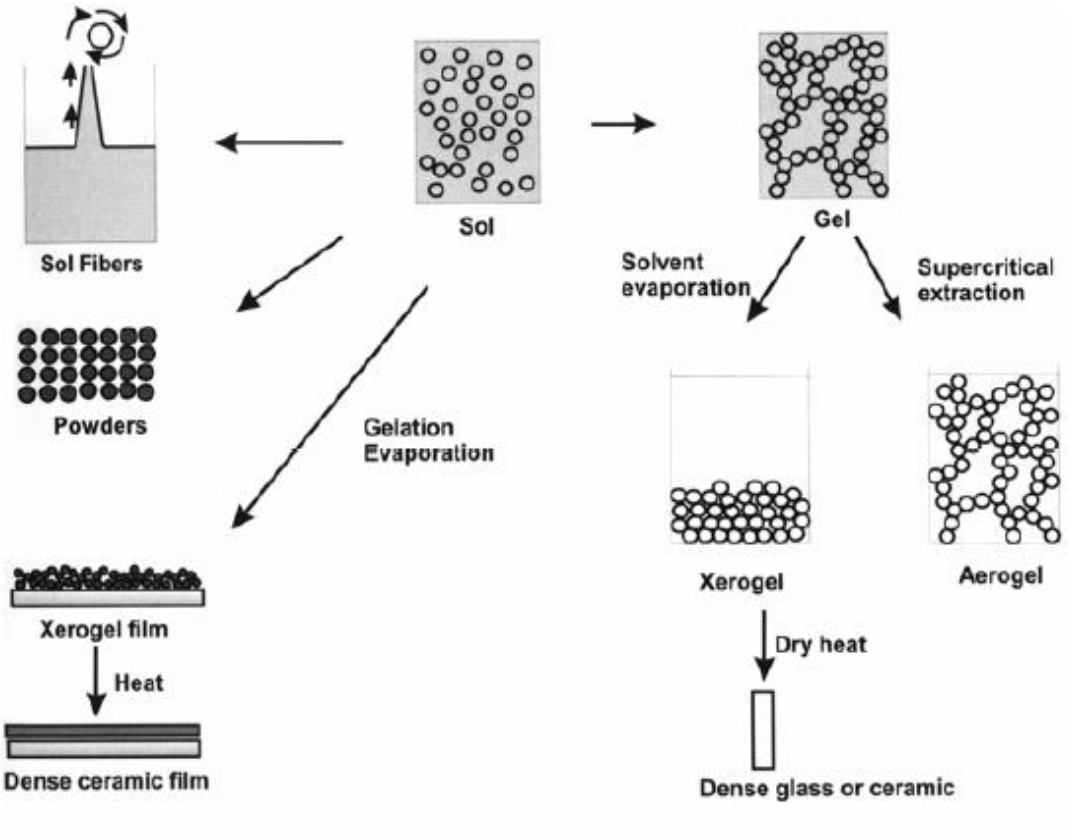

Figure 2.1 Sol processing Option

2.3 Aim of work

As demonstrated by literature review functional materials have been investigated to show interesting unique properties like electronic, semiconducting, piezoelectricity etc. Among these metal oxides family, particularly Zinc oxide is interesting material among scientific community, because of the commercial importance as thin films for SAW base as well as chemo-resistive gas sensor. The main aim of the work is to obtain the perfect structural as well as optical characteristics for the ZnO based thin film that can be used in chemo-resistive gas sensor. Further we will analysis the effect of variations in parameters like molarity and thickness contributing towards energy band gap and its effect for sensing properties.

The prime objectives are:

1. **Annealing Temperature Optimization for Highly Crystalline Thin Films**
2. **Study of Particle Size and Energy Band Gap Variation with Molarity Concentration Variation.**
3. **Study of Effects over Gas Sensing Properties.**

Further studies will be done according to the derived objectives. At first, the sample will be studied for annealing temperature optimization such that each sample prepared for further studies will be pure crystalline form of ZnO thin films.

Chapter 3

Methodology and Characterization techniques

This chapter deals to the method adopted for ZnO thin film deposition and characterization techniques for thin film deposition.

3.1 Materials

As studied in literature Zinc Oxide (ZnO) can be prepared through chemical route by using various chemicals like Zinc Nitrate Hexahydrate, Zinc Acetate dihydrate with solvent like IPA, Methnol and Ethanol. As discussed by [29, 33, 36], the following materials have been used for the synthesis of ZnO:

1. Zinc Acetate Dihydrate (Zn $(CH_3COO).2H_2O$)
2. Ethanol (C_2H_6O)
3. Monoethanolamine ($HOCH_2CH_2NH_2$)

The materials used for Cleaning of subtract

1. Trichloroethylene(C_2HCl_3) (TCE)
2. Acetone (C_3H_6O)
3. Isopropyl alcohol (C_3H_8O)

3.2 Cleaning of substrate

RCA2 procedure has been followed for cleaning substrate as discussed below:

3.2.1 Preparation of RCA2

This process requires 20 minutes for complete. The recipe for RCA2 is : 6 parts DI (D Ionized) water (H_2O), 1 part Hydro chloride Acid(HCl), 1 part of Hydrogen per Oxide (H_2O_2).

300ml of H_2O

50ml HCl

50ml H_2O_2

3.2.2 Procedure of RCA2

In a Pyrex beaker put 300ml DI water. Add 50ml of HCl in this water and heat up to 70°C to 75°C on hot plate. Take out this solution from hot plate and add 50ml of H_2O_2. This solution will bubble for 1 to 2 minute, which indicate solution is ready for cleaning. Sock the substrate in this solution for 15 minutes to 20 minutes. Remove this substrate from solution and wash with clean DI water.

3.3 Substrate Used

1. Glass
2. Silicon
3. Quartz

3.4 Synthesis of ZnO samples:

3.4.1 Preparation of solution

All the materials were weight by electronic weighing balance. The liquid materials measure by measuring cylinder. For desired molarity weighed Zinc acetated dihydrate is dissolved in particular amount of liquid Ethanol. The solution is put on hot plate with Magnetic stirrer.

For easily dissolving the temperature of hot plate was kept at 60°C and rpm was maintained between 400rpm to 600rpm.The Monoethanolamine (MEA) as stabilizing agent was added drop by drop during rotation. Molar ratio of MEA to zinc acetate dihydrate was set to 2. The stirrer procedure continued for 45 minutes to 60 minutes. After that the solution was kept at room temperature for 12-24 hours to check ageing effect and polymers network formation.

3.4.2 Cleaning Process

The Substrate was first cleaned with Deionized water and Dried with Nitrogen Gas or on a hot plate. The cleaning was followed by Trichloroethylene, Acetone and Isopropyl alcohol used to remove inorganic impurity, organic impurity, and residues of Trichloroethylene and Acetone respectively.

3.4.3 Thin film deposition

Ultra clean substrate is put on substrate holder in spin coater as shown in figure 3.1. The vacuum is generated by vacuum pump which holds substrate during rotation and does not allow to fell it down. A program which related to RPM speed and RPM's time is set in spin coater. A drop of precursor solution is dropped on substrate and run the program for uniformly spreading of solution on substrate. After program completion, the substrate is put on hot plate at high temperature for baking. Baking is done for evaporation of the solvent. The time duration for baking is 3-5 minutes. The whole procedure is repeated to achieve the desired thickness. After this substrate is put for annealing in closed environment using muffle furnace at desired annealing temperature for some time duration.

The samples prepared for the further study are elaborated and denoted with their code names as describe below:

Sample S-A

Substrate: Glass

Molarity :1M

Volume of solution : 60ml

Weight of Zinc Acetate Dihydrate: 13.17gram

Annealing Temperature: 300°C

Duration of Annealing Temperature: 12 hrs.

Sample S-B

Substrate: Glass

Molarity :1M

Volume of solution : 60ml

Weight of Zinc Acetate Dihydrate: 13.17gram

Annealing Temperature: 400°C

Duration of Annealing Temperature: 12 hrs.

Sample S-C

Substrate: Glass

Molarity :1M

Volume of solution : 60ml

Weight of Zinc Acetate Dihydrate: 13.17gram

Annealing Temperature: 500°C

Duration of Annealing Temperature: 12 hrs

Sample S-D

Substrate: Glass

Molarity :1M

Volume of solution : 60ml

Weight of Zinc Acetate Dihydrate: 13.17gram

Annealing Temperature: 600°C

Duration of Annealing Temperature: 6 hrs

Sample S1

Substrate: Silicon

Molarity :1M

Volume of solution : 60ml

Weight of Zinc Acetate Dihydrate: 13.17gram

Annealing Temperature: 600°C

Duration of Annealing Temperature: 6 hrs

Sample S2

Substrate: Silicon

Molarity :0.7M

Volume of solution : 60ml

Weight of Zinc Acetate Dihydrate: 9.219 grams

Annealing Temperature: 600°C

Duration of Annealing Temperature: 6 hrs

Sample S3

Substrate: Silicon

Molarity :0.5M

Volume of solution : 60ml

Weight of Zinc Acetate Dihydrate: 6.585 grams

Annealing Temperature: 600°C

Duration of Annealing Temperature: 6 hrs

Sample S4

Substrate: Silicon

Molarity :0.33M

Volume of solution : 60ml

Weight of Zinc Acetate Dihydrate: 4.3461 grams

Annealing Temperature: 600°C

Duration of Annealing Temperature: 6 hrs

Sample S5

Substrate: Silicon

Molarity :0.1M

Volume of solution : 60ml

Weight of Zinc Acetate Dihydrate: 1.317 grams

Annealing Temperature: 600°C

Duration of Annealing Temperature: 6 hrs

Sample S6

Substrate: Silicon

Molarity :0.05M

Volume of solution : 60ml

Weight of Zinc Acetate Dihydrate: 0.6585 grams

Annealing Temperature: 600°C

Duration of Annealing Temperature: 6 hrs

The thickness is not monitored for any sample as we have taken a single coat of each solution for the preparation of each sample.

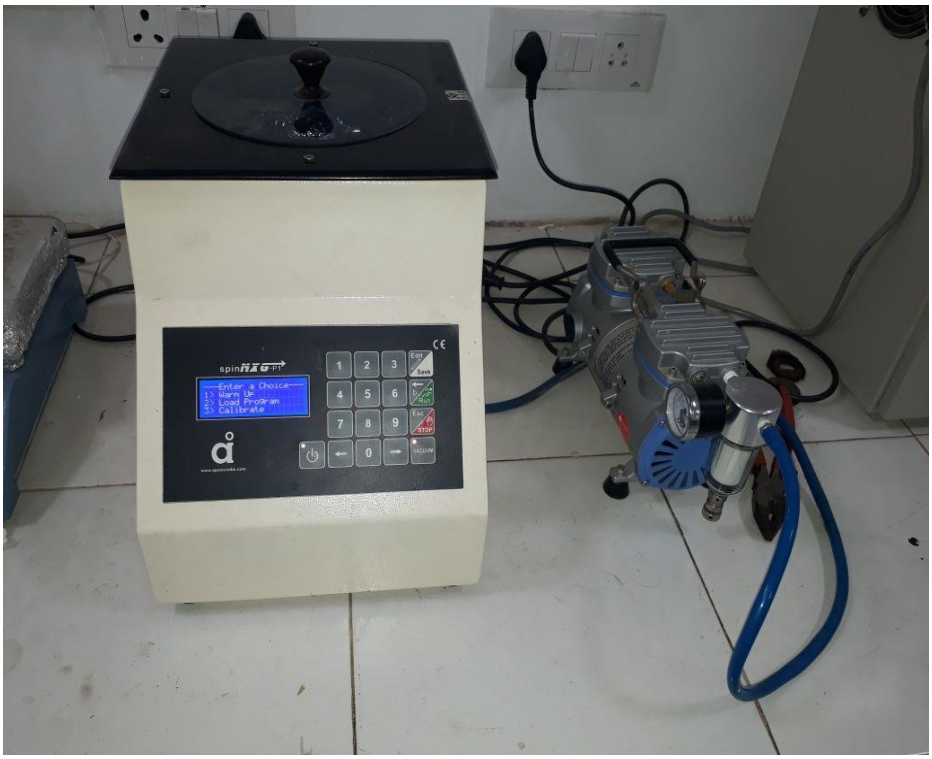

Figure 3.1 Spin Coater

3.5 Characterization techniques

3.5.1 X-ray Diffraction

X-ray diffraction (XRD) is one of the versatile, non-destructive technique which is used for qualitative and quantitative analysis of a crystalline materials. This characterization technique is used to determine the overall structure of bulk solids. This experimental technique is used for identification of unknown materials. By using this technique orientation of single crystals and orientation of polycrystalline can be found out. It is helpful technique to determine stress, texture and thickness of films. For this study, X ray is used of Cu-K alpha x-ray tube of wave length (λ)=1.54056 A°. The X ray scans were performed 20°to 60° with a typical step size of about 0.1°[20, 35, 37].

- **Generation of X -ray**

X rays are short wavelength electromagnetic waves that possesses high energy of electromagnetic radiation. It has properties of both the waves and particles which can be described in terms of both photon energy (E) or wavelength, λ and frequency ν. The relation between photon Energy and frequency is given in equation 3.1

$$E = h\nu \quad (3.1)$$

$$\& \quad c = \lambda\nu \quad (3.2)$$

Where h, ν, c are plank constant, frequency, velocity of Electromagnetic wave.

X-rays are generated whenever electrons with very high energy strike with metal target. Any type of x-ray generation tube must contain (I) a source of electron (II) a high accelerating voltage (III) a metal target.

All x-ray tubes contain two electrodes which are an anode (the metal target) usually maintained, at ground potential, and a cathode maintained, at negative potential, normally of order of 30KV to 50KV for the diffraction work. Interaction that occur between the beam (i.e. electron) and target will result in a loss of energy. A continuous spectrum is produced when the high energy electrons are slowed down rapidly by multiple collisions with the anode material, which give rise to white radiation, or so-called Bremsstrahlung.

Because of rapid deceleration of the electrons hitting the target, as mentioned above a continuous spectrum is formed. In this scenario every electron does not decelerate in the same way, some stop in one impact and release all their energy at once, while other deflect this way and that when they encounter atoms of the target, successively losing fractions of their total kinetic energy until is all spent. Those electrons which are stopped in one impact become reason of producing photons of maxim energy (wavelength) equal to the energy loss[37].

- **Bragg's Law**

Since atoms are periodically arranged in a lattice, Scattered x-rays from a crystalline solid can constructively interfere, producing a diffracted beam through these atoms. A predictable relationship among several factors was recognized by W. L. Bragg. These factors are combined in Bragg's law which is given in equation 3.3

$$n\lambda = 2d \sin\Theta \quad (3.3)$$

n = an integer

λ = the wavelength of the incident X-radiation (for this study 0.154 angstroms)

d = the distance of inter atomic planes

θ = the diffraction angle in degree

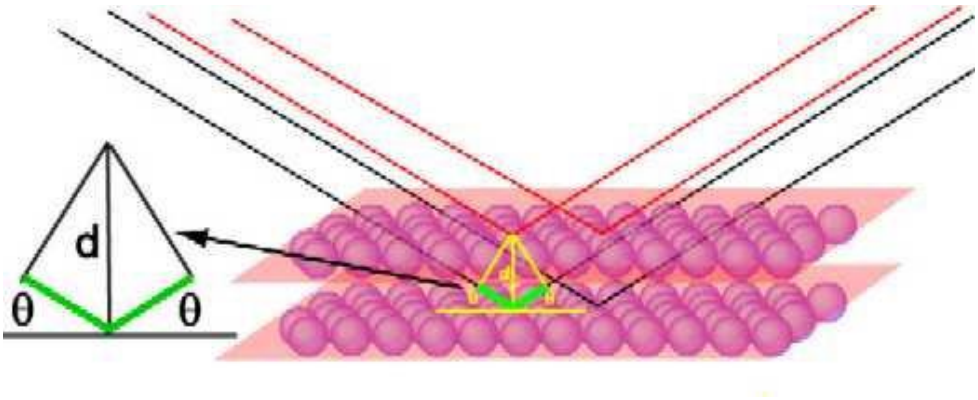

Figure 3.2 Bragg's diffraction condition.

- **Crystallite size measurement**

Identification of phase of the peaks by using xrd depends on the positions in a diffraction profile as well as the relative intensities of these peaks to some extent. Another aspect of the diffraction which comes under consideration from material is to consider how diffraction peaks are varied in the presence of various types of defects such as small number of dislocations in crystals with dimensions of millimetres. Small size of grains can be considered as another kind of defect and can change width of diffraction peak . Peak broading comes due to small size crystal. The crystallite size is a function of peak width (specified as the full-width at half maximum peak intensity (FWHM)), peak position and wavelength. Crystallite size can be easily calculated using Scherrer's formula which is discussed below. [37-41]

- **Scherrer's formula**

It is given by Paul Scherrer. Scherrer's relation is used to determine crystallite size in X-ray diffraction and crystallography.

Scherrer's formula is written as:

$$D = \frac{0.94\,\lambda}{B\cos\theta} \tag{3.4}$$

Where λ, θ and B are the X-ray wavelength, Bragg's diffraction angle and FWHM of the ZnO diffraction peaks, respectively[37] .

3.5.2 UV -visible spectroscopy

It is a most significant technique to study the band structure of the semiconductors. Band structure of semiconductor can be determined directly and easily by calculating the absorption spectrum. Absorption is expressed in terms of a coefficient hv, that is proportional to the energy gap Eg. The optical absorption coefficient depends on the energy of incident photon and determined by Equation 3.5:

$$\alpha h\nu = A\left(h\nu - E_g\right)^{1/2} \tag{3.5}$$

Where A is a constant, h is the planks constant, and ν is the frequency of the incident beam. Solutions of transition metal ions are coloured and absorb light of specific wavelength. The colour of such metal ion solutions is strongly affected by the addition of other species like anion and ligands. Because of these kinds of impurities, the colour of the solution changes and wavelength of maximum absorption also changes[24, 40, 42].

3.6 Gas Sensing Set-up: A sensing set up was assemble. It consists the following assemble

1. Vacuum Chamber
2. Temperature Controller
3. Digital multimeter

Vacuum Chamber: In this chamber vacuum can be created using two pumps:

(a) Rotary Pump

(b) Diffusion pump

Rotary pump first creates rough vacuum. After creating rough vacuum deep value of vacuum is achieved by diffusion pump. Sample under test is put on sampler holder. Surface of sample holder is connected to heater. Heater is used to hot surface of sample holder to activate adsorption and desorption of gas molecules.

Temperature Controller: It is used to maintained temperature of surface of sample holder. It is connected in feedback connection to heater. When temperature of surface of sample holder crosses certain amount of temperature, it disconnected heater to power supply and when temperature of surface of sample holder falls down then it connects heater to power supply and temperature of surface of sample holder again starts to rise.

Digital Multimeter: It is used to measure resistance of sample under test. It is connected in parallel topology with sample. When resistance of sample under test changes due to adsorption and desorption of gas molecules, it shows value of changed resistance due to gas molecules.

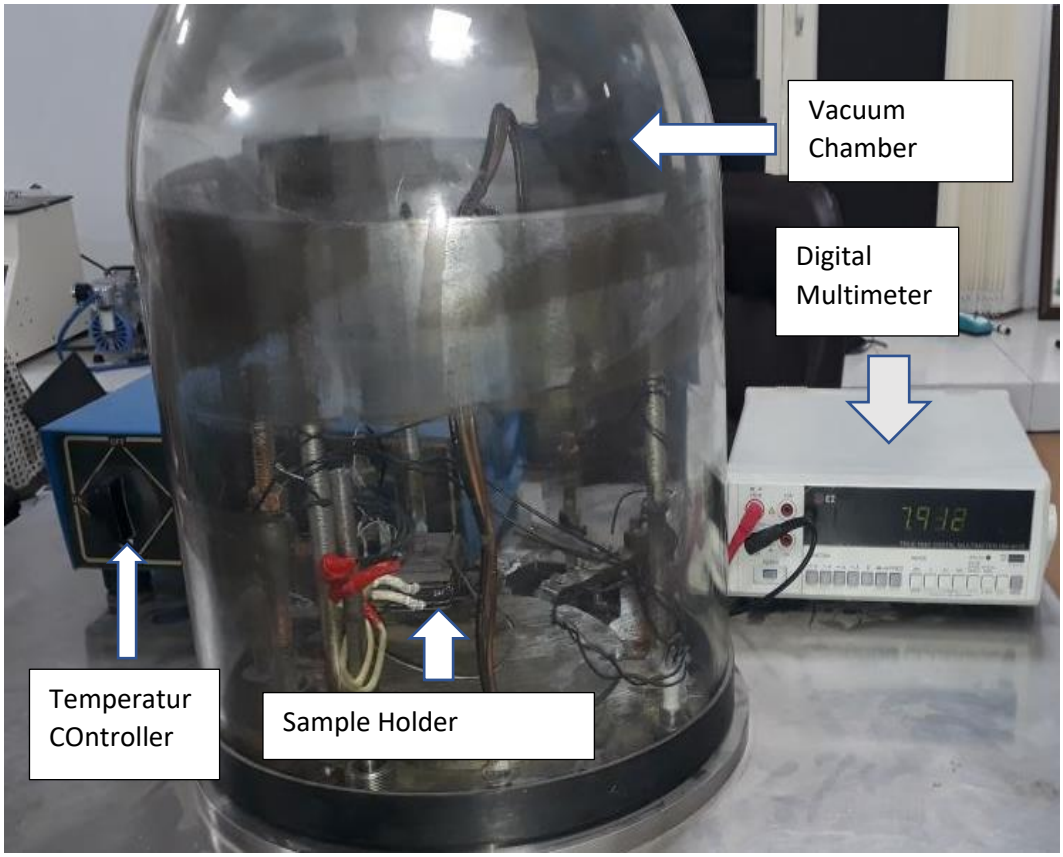

Figure 3.3 Gas Sensing set up

As shown in Figure 3.3, the gas sensing set up has been used for the sensing results for the prepared sensor. The reading from Digital multi meter has be carefully recorded manually over per second basis and hence used for the further calculations for the sensitivity and response time and recovery time.

3.7 Conclusion

In this chapter we have discussed about Methodology to synthesis ZnO thin film, material used. In this chapter we discussed about characterization techniques and their use in synthesis of ZnO thin film. We mention a gas sensing set up also in this chapter.

Chapter 4

Results and Discussion

This chapter deals to results obtained from X-rd analysis, UV-visible Spectroscopy. The obtained results we will discuss about crystallite size, energy band gap and sensitivity, response time and recovery time of sample.

Sample S-A

The Xrd result of sample S-A shown in Figure 4.1. From this XRD result it is clear that ZnO synthesized is purely amorphous and the single peak at 31.40656° represents either the base of the substrate holder of XRD setup or some other noisy signal. The highest peak in figure 4.1 comes due to metal.

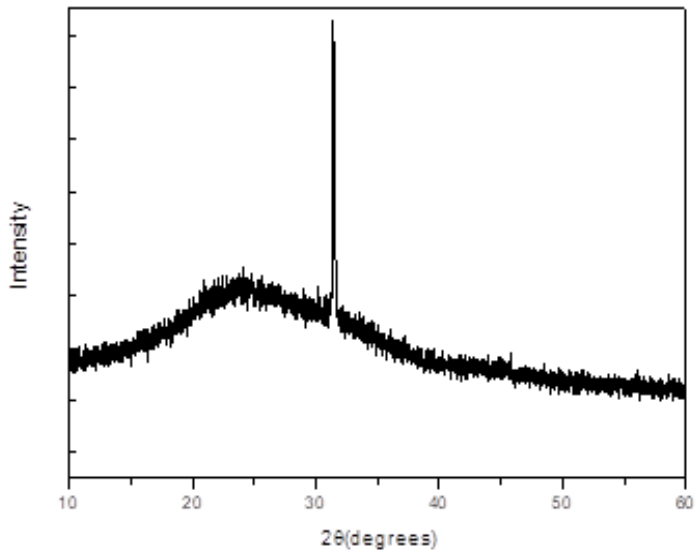

Figure 4.1 Xrd result of Sample S-A

Sample S-B

Figure 4.2 represents the xrd result of sample S-B. It can be concluded from this Xrd result that ZnO deposited is still highly amorphous in nature.

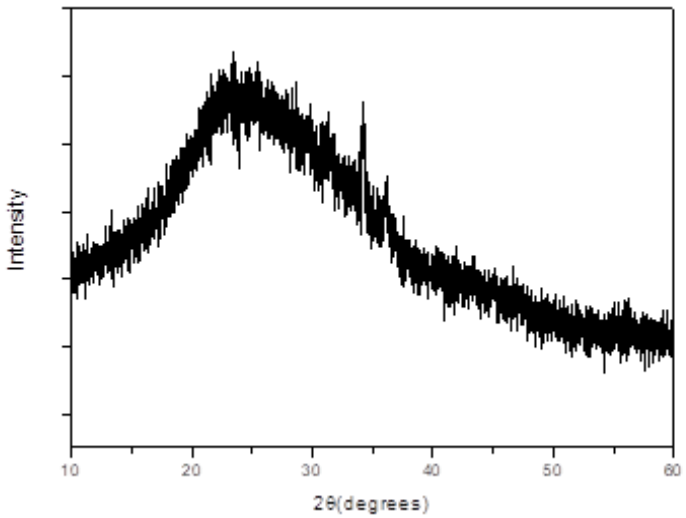

Figure 4.2 Xrd result of Sample S-B

Sample S-C

The Xrd result of sample S-C in Figure 4.3 shows that ZnO is still highly amorphous with some crystalline structures formed within the sample. The hump represents the substrate of the sample prepared.

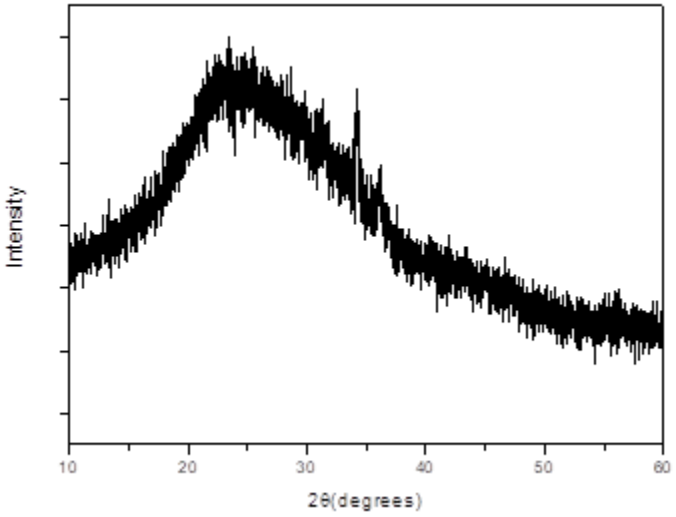

Figure 4.3 Xrd Result of sample S-C

Melting temperature of Glass substrate which we used is around 525°C. So we changed substrate which have higher melting temperature.

Sample S-D

The Xrd result of sample S-D shown in figure 4.4. It can be clearly stated that ZnO has been formed at 600°C with proper crystalline structure. So we counited further with annealing temperature 600°C. The required peaks for ZnO in Xrd has come at 32.12809°, 34.78041°, 36.59239° represents 100, 002, 101 planes respectively. The plane 101 has dominant intensity over 100, 002, 101 planes.

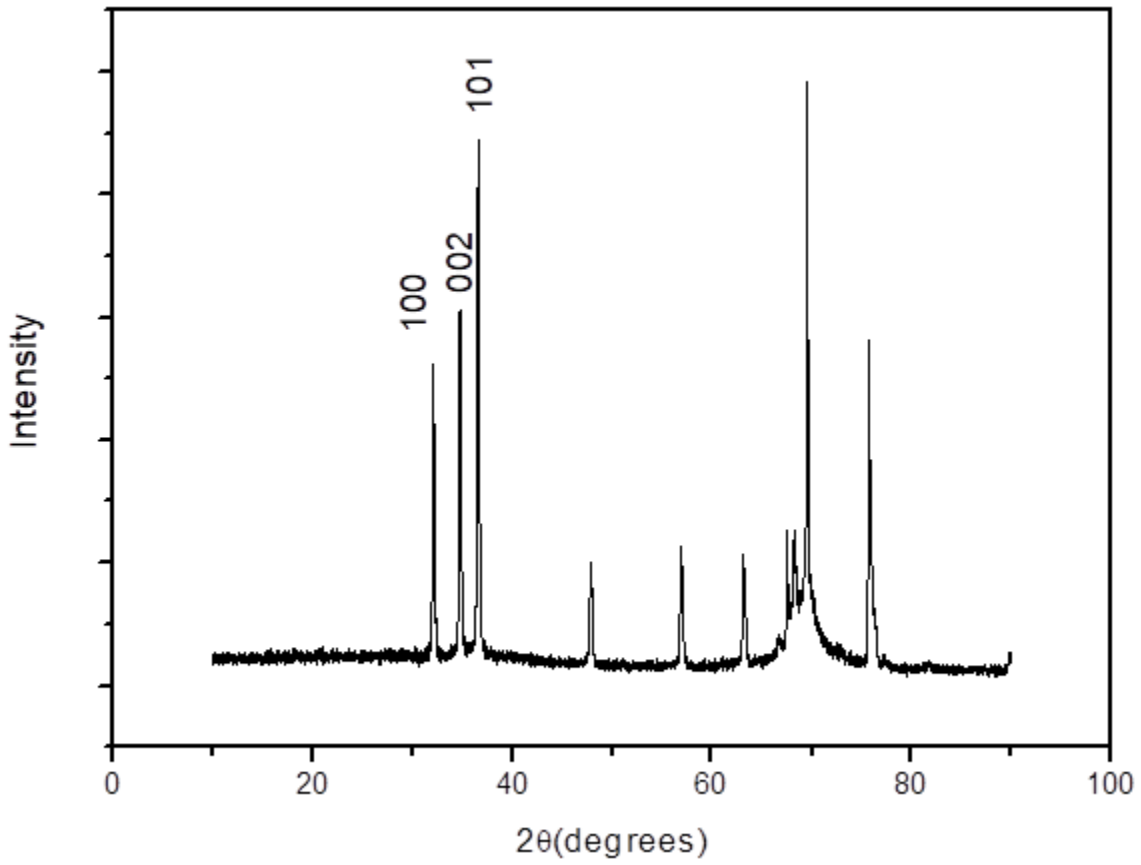

Figure 4.4 Xrd Result of sample S-D

The Xrd results for all the samples S1, S2, S3, S4, S5, S6 is as shown in Figure 4.5. This result is compared with standard JCPDS No. 36-1451. Now from this result this can be concluded that a highly crystalline thin film of ZnO has been fabricated at 600°C. Hence for further studies annealing temperature is kept constant at 600°C which will enable us to show the difference between the samples with other changing parameters.

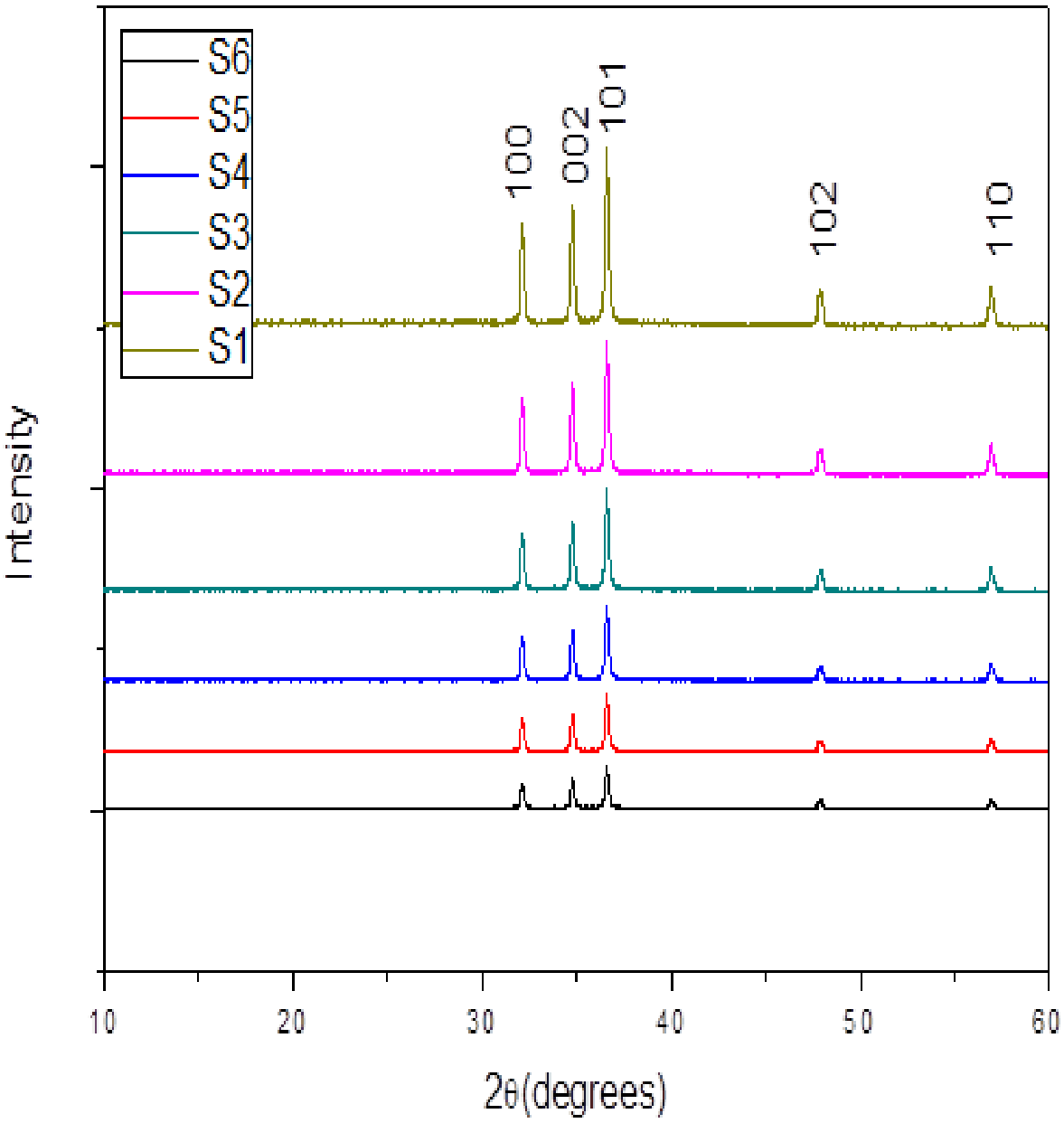

Figure 4.5 Xrd pattern of the ZnO films for sample S1, S2, S3, S4, S5, S6 ZnO Molarity Concentration

Table 4.1 – Crystallite size calculations using Scherrer's formula.

Sample coding	Peak position 2θ (°)	FWHM B size (°)	Dp (nm)
S1(1M)	36.60000	0.24412	37.79
S2(0.7M)	36.60006	0.24047	37.16
S3(0.5M)	36.60008	0.23842	37.02
S4(0.33M)	36.60012	0.23616	36.67
S5(0.1M)	36.60015	0.23527	36.36
S6(0.05M)	36.60021	0.23136	35.81

Figure 4.5 shows the XRD graph for all six samples. ω–2θ scans by using a fixed grazing incidence (ω =1°) yield the diffraction patterns showed in figure 4.5. As from figure 4.5, all of the six samples indicate preferential orientation along c-axis. The peaks are identified to planes 100,002,101,102,110 for a single-phase wurtzite ZnO structure. The 101 plane has the dominant intensity over all planes of all samples. The diffraction peaks of XRD result are compared with a pure hexagonal wurtzite structure (JCPDS No. 36-1451) for ZnO. As molarity increases, peaks of XRD also increases shown in figure 4.5. It can be revealed that molarity of precursor solution indicates a number of moles present in solution. As sol molarity increases, the number of moles also increases which causes increase in thickness of the film and hence crystallite size also increases.

XRD graphs clearly indicate that increase in the crystallite size with the increase in molarity of the ZnO thin film layer as shown in figure 4.5 using Scherrer's relation average crystallite size is calculated. It can be clearly stated from the results that increase in molarity causes increase in crystallite size. The crystallite size (average grain size) of the ZnO thin films varies from 35.81nm to 37.79 nm with an increase in molarity concentration of ZnO from 0.05M to 1M as mention in Table 4.1. The minimum average crystallite size (grain size) of Sample S6 is 35.81nm and maximum crystallite size (grain size) of sample S1 is 37.79nm.

4.1 Gas sensing properties

The gas sensing experiments have been performed for all six samples. Figure 4.6 represents sensitivity response changes with a change in temperature for all samples towards NOx gas. Sample S6 (0.05M), S4 (0.33M), S3 (0.5M), S2 (0.7M), S1 (1M) show their highest sensitivity 77%, 76%, 71%, 68%, 67% respectively at optimum temperature of 300°C. Sample S5 having molarity 0.1M shows the highest sensitivity 80% among all the samples at 300°C. According to this study, optimum molarity concertation for NOx gas sensing comes out to be 0.1M. It can be stated that optimum highest sensitivity response of

the sample S5 (0.1M) is because of perfect average crystallite size (defects created) obtained at 0.1M. Surface roughness increases with increase in sol molarity hence increased surface roughness causes increase in the surface to volume ratio. The sample S5 (0.1M) has the best surface to volume ratio which shows highest sensitivity response at optimum temperature towards NOx gas. From figure 4.6, sample S5 (0.1M) has higher sensitivity response than sample S6 (0.05M) and sensitivity response of all other samples except sample S5 and sample S6 are low as their sol molarity is high. It can be stated that sensitivity response first increases with increase in sol molarity but after a certain molarity concentration sensitivity response starts to decrease as sol molarity increase.

The sensitivity response increases with increase in temperature after a certain temperature sensitivity response decreases. The explanation of this phenomenon is studied using the kinetics of molecules [43-45]. At low operating temperature, the kinetic energy of a gas molecule is not sufficient that cannot react to a central active layer of sensing sample hence results in a low rate of adsorption. The low rate of adsorption further causes to low sensitivity response. When this operating temperature is increased sensitivity increases because of increase in the rate of adsorption rate of gas molecules on sensing samples. When this operating temperature crosses the certain limit of increment, the kinetic energy of the gas molecules also increases in such a way that the molecules will escape before reacting with the active sensing layer again resulting in lowered desorption rate of gas molecules at the surface of the sensing layer hence it results in low rate of adsorption [46]. The low rate of adsorption causes low sensitivity above and below the optimum temperature.

Response time and recovery time are described in Figure 4.7, Figure 4.8, Figure 4.9, Figure 4.10, Figure 4.11, Figure 4.12 of sample S6(0.05M), S5(0.1M), S4(0.33M), S3(0.5M), S2(0.7M), S1(1M) respectively. These graphs show that there is continuously almost linear decrement with the rise in operating temperature. This decrease in response time and recovery time is again explained by kinetic of molecules [46]. For optimum response time and recovery time adsorption rate and desorption rate should be high.

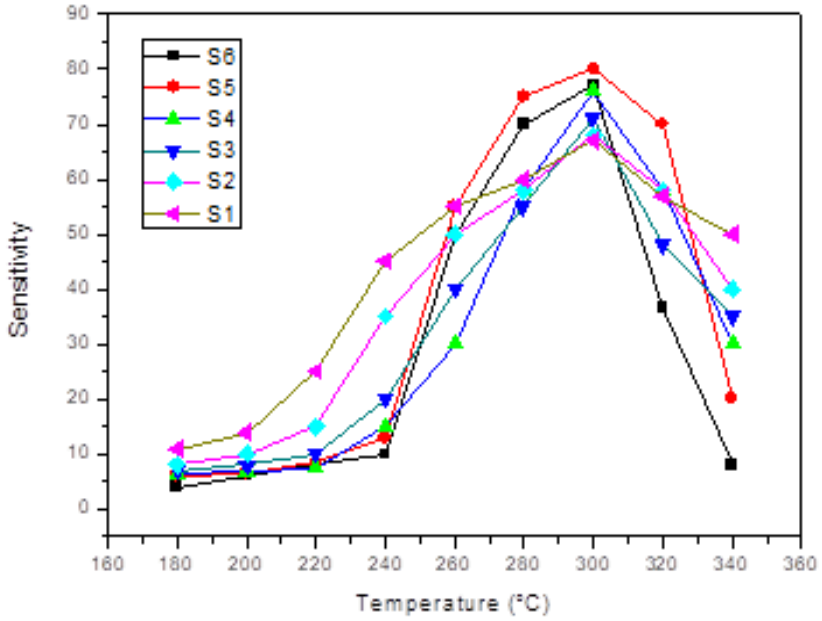

Figure 4.6 Sensitivity vs Temperature

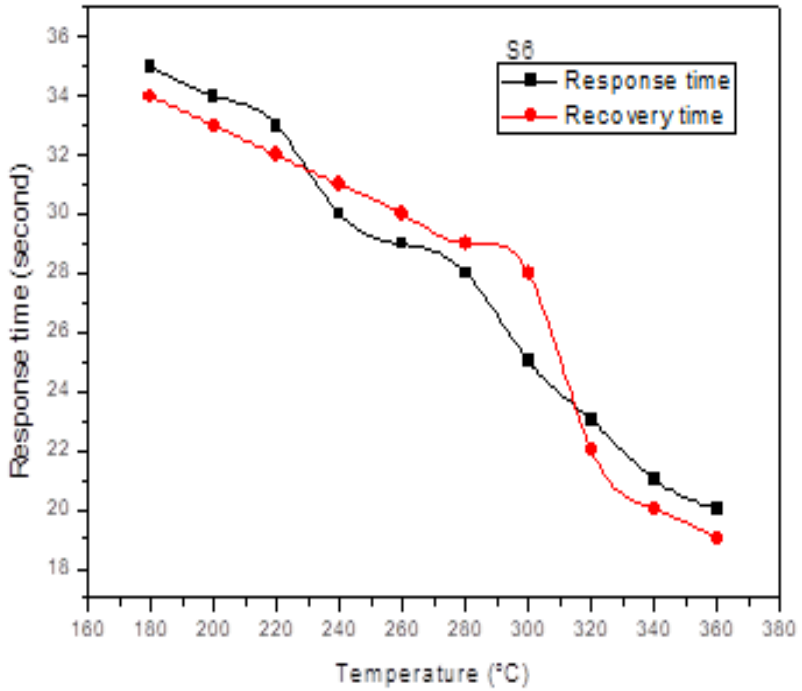

Figure 4.7 Response time vs Temperature of sample S6

Figure 4.7 explains the minimum response time and minimum recovery time of sample S6(0.05M) is 25 seconds and 28 seconds respectively at an optimum temperature of 300°C.

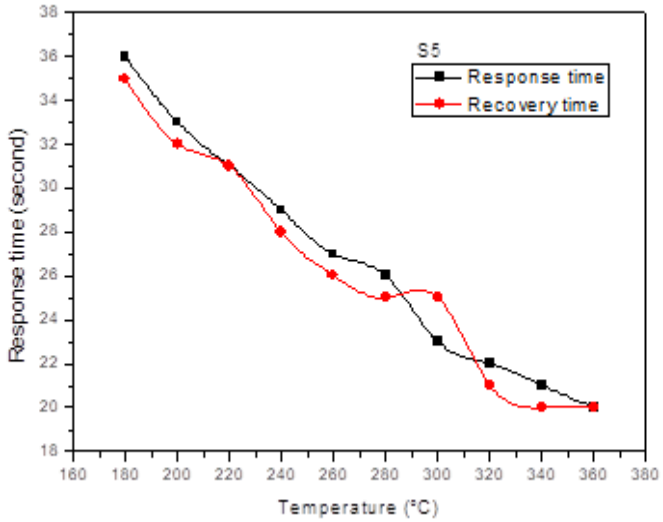

Figure 4.8 Response time vs Temperature of sample S5

It is clear from figure 4.8 that minimum response time and minimum recovery time of sample S5(0.1M) at an optimum temperature of 300°C is 23 seconds and 25 seconds respectively.

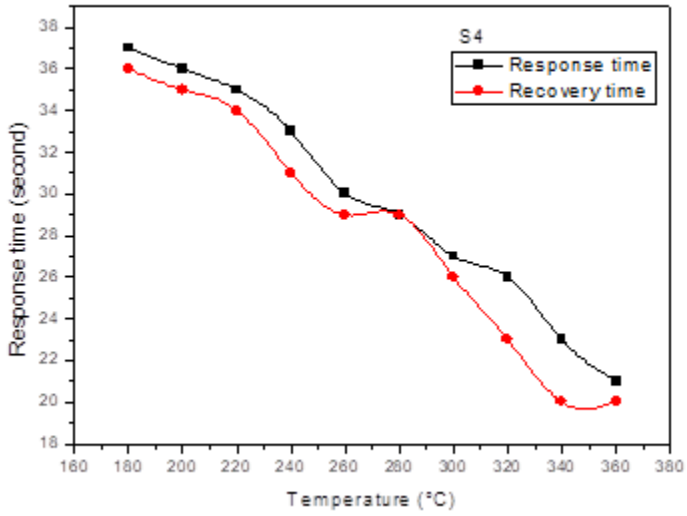

Figure 4.9 Response time vs Temperature of sample S4

It can be stated from Figure 4.9 that minimum response time is 27 seconds and minimum recovery time is 26 seconds for sample S4(0.33M) at 300°C optimum temperature.

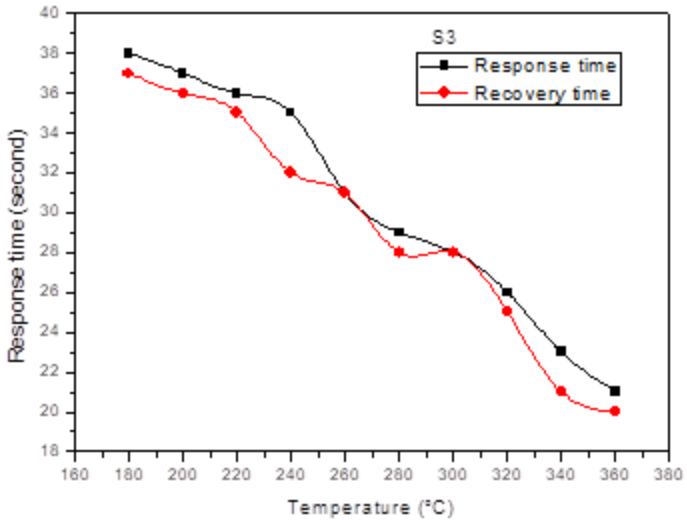

Figure 4.10 Response time vs Temperature of sample S3

The value of minimum response time and minimum recovery time of sample S3 from Figure 4.10 are same which is 28 seconds at optimum temperature 300°C.

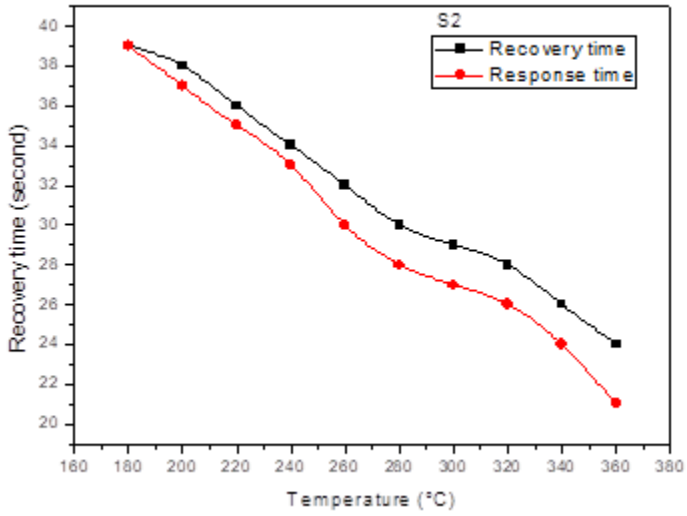

Figure 4.11 Response time vs Temperature of sample S2

Figure 4.11 shows at optimum temperature 300°C the value of minimum response time and minimum recovery time of sample S2(0.7M) is 29 seconds and 27 seconds.

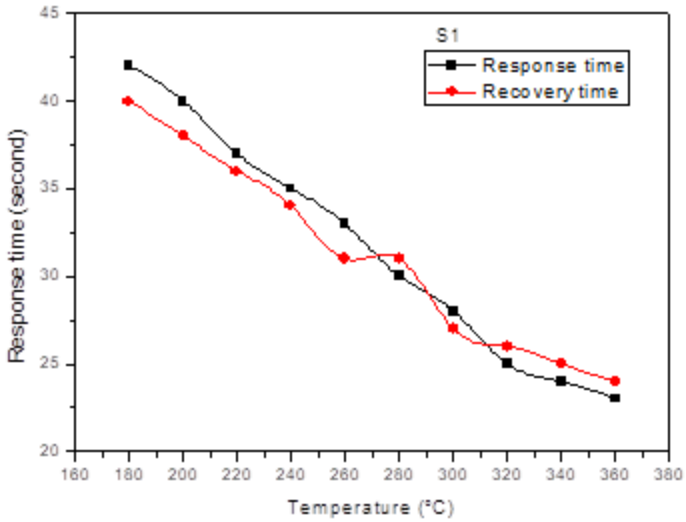

Figure 4.12 Response time vs Temperature of Sample S1.

Figure 4.12 gives the minimum response time and minimum recovery time of sample S1(1M) is 28 seconds and 27 seconds at optimum temperature 300°C respectively.

It can be stated from above study that Sample S5(0.1M) has minimum response time 23 seconds and minimum recovery 25 seconds at optimum temperature 300°C among all sensing samples. The reason behind this is Sample S5(0.1M) has perfect average crystallite size for sensing.

4.2 Variation in Energy band gap of ZnO with Molarity Variation.

We have prepared the single coated samples as S1, S2, S3, S4, S5, S6 with different molarities of 1M, 0.7M, 0.5M, 0.33M, 0.1M, 0.05M respectively. From UV plot and Tauc plot, Energy band gap of each sample is calculated for which the results are discussed below. The UV graphs are plotted through the transmittance factor denoted by %T and wavelength denoted by λ which is nano meter. From UV graphs Tauc plot are drawn in which x axis shows energy of photons and y axis shows absorption coefficient $(\alpha h\nu)^2$.

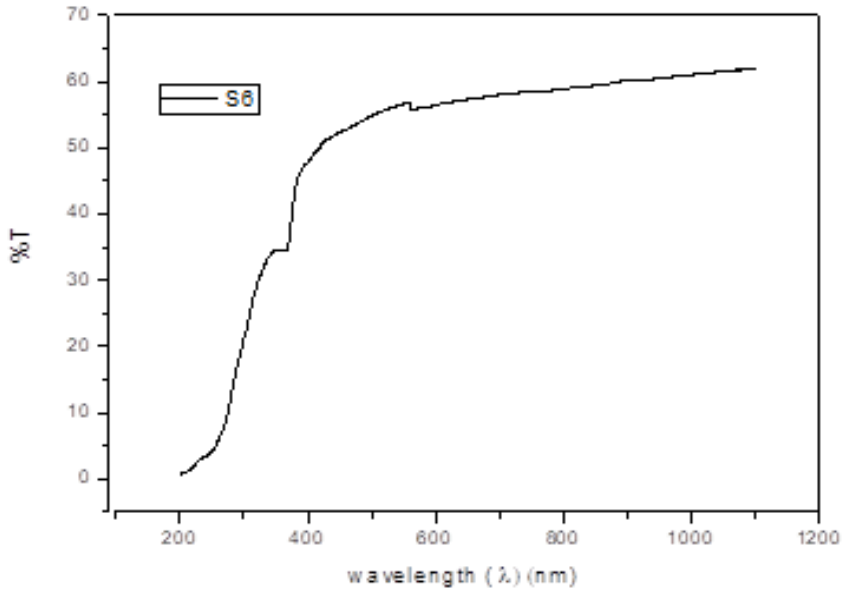

Figure 4.13 UV graph of sample S6

From figure 4.13 maximum percentage of transmittance of sample S6 is approximately equal to 61.85%.

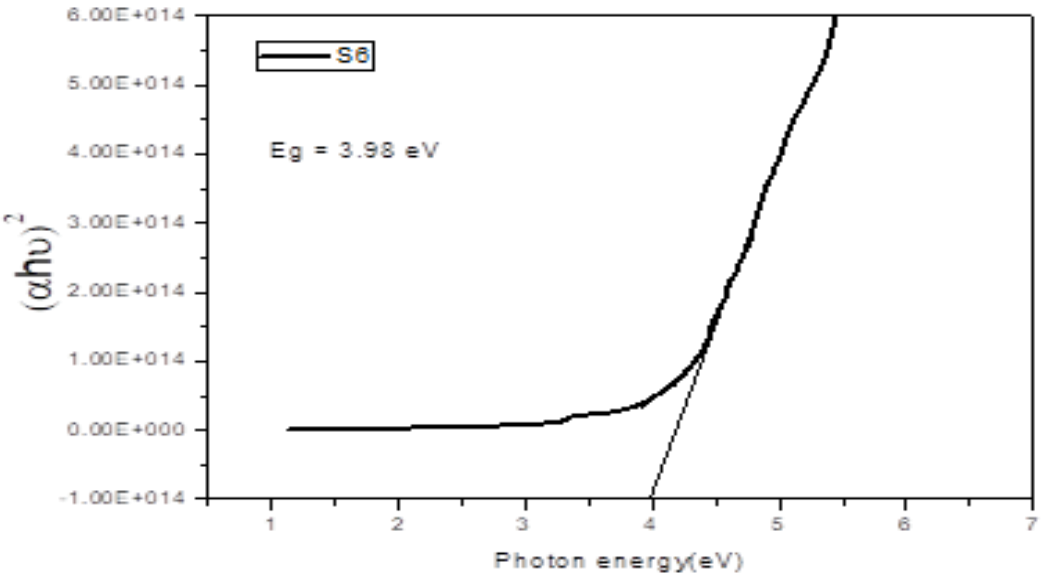

Figure 4.14 Tauc plot of sample S6

From Figure 4.14 the energy bandgap of sample S6 is 3.98 eV.

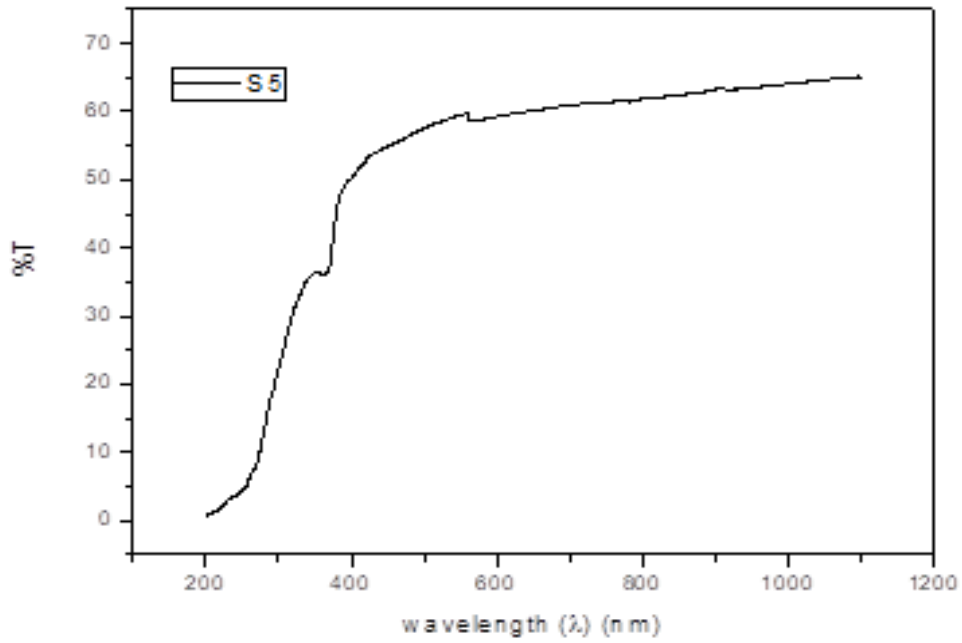

Figure 4.15 UV graph of sample S5

From Figure 4.15 maximum percentage transmittance of sample S5 is approximate equal to 65.19 % .

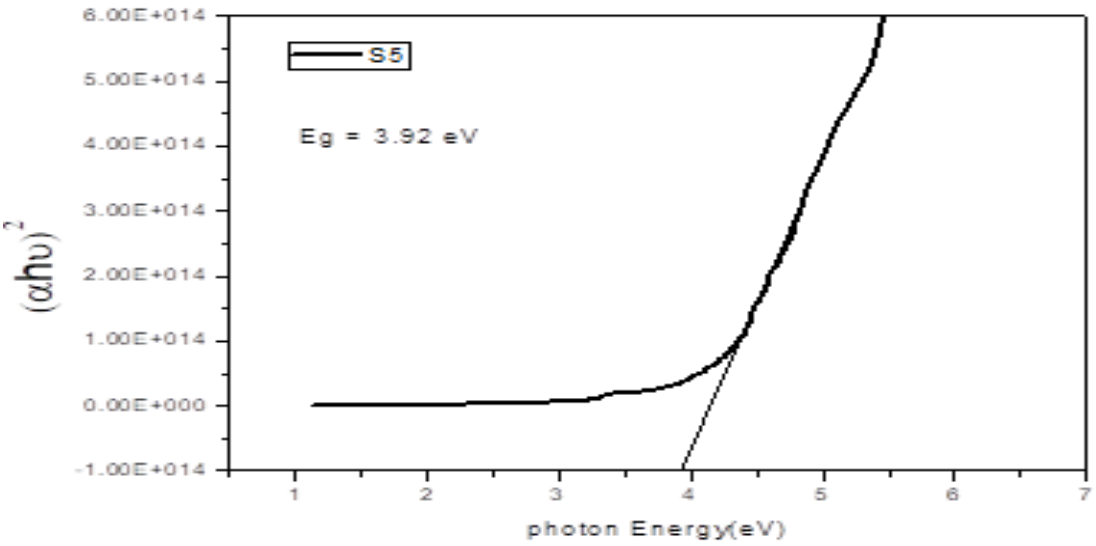

Figure 4.16 Tauc plot of sample S5

The energy bandgap of sample S5 is 3.92 eV as shown in Figure 4.16.

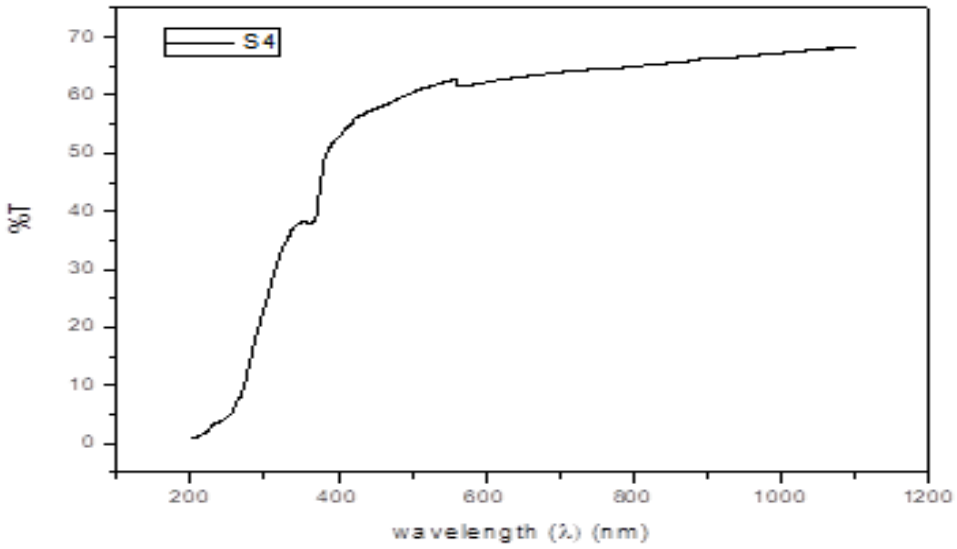

Figure 4.17 UV graph of sample S4

From Figure 4.17 maximum percentage transmittance of sample S4 is approximately equal to 68.28%.

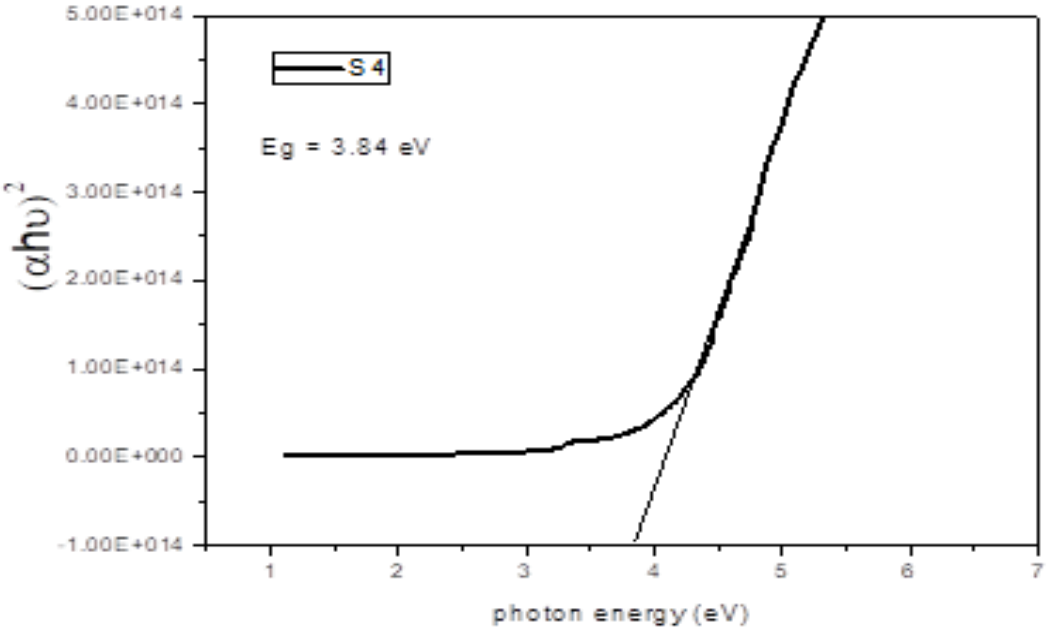

Figure 4.18 Tauc plot of sample S4

The energy band gap of sample S4 from Figure 4.18 is 3.84 eV.

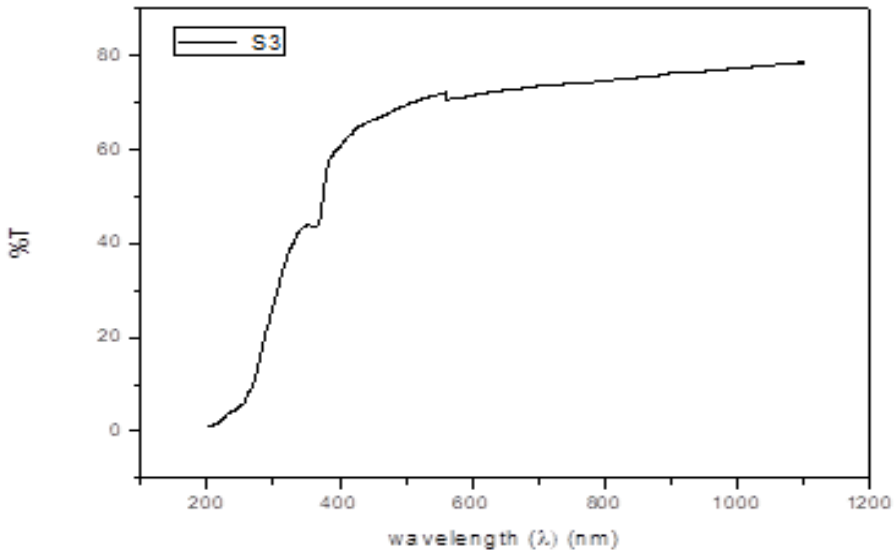

Figure 4.19 UV graph sample S3

From Figure 4.19 maximum percentage transmittance of sample S3 is approximately equal to 78.44%.

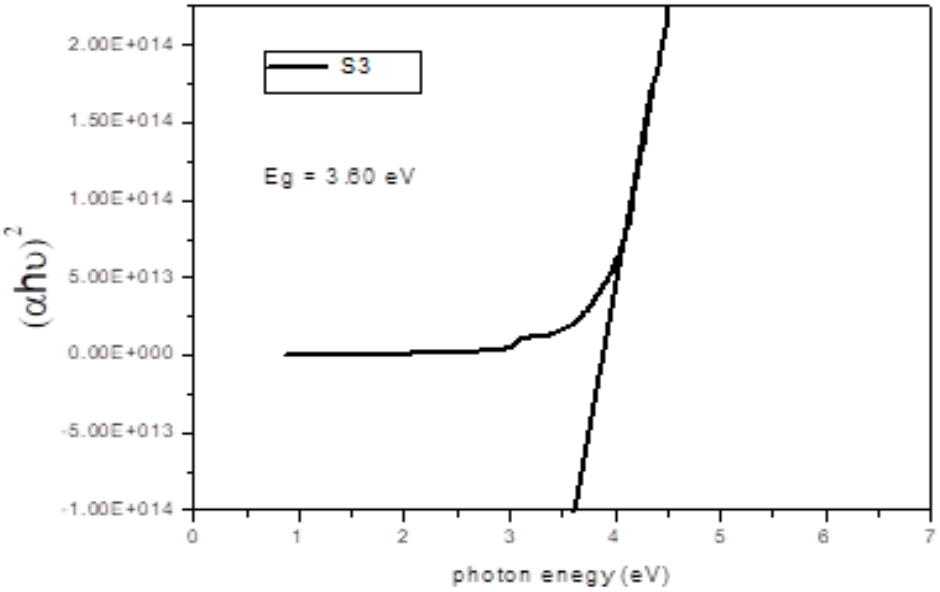

Figure 4.20 Tauc plot of sample S3

From Figure 4.20 the energy band gap is 3.60 eV of sample S3.

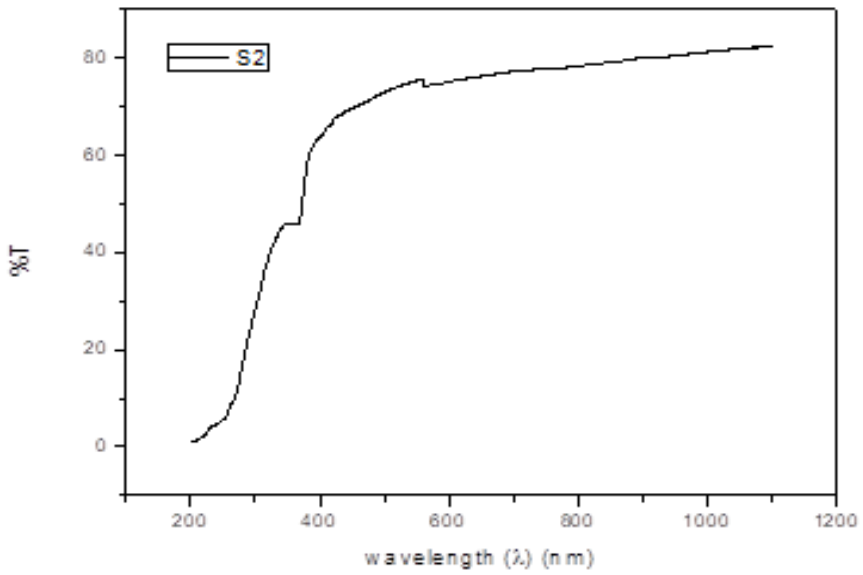

Figure 4.21 UV graph of sample S2

From Figure 4.21 maximum percentage transmittance of sample S2 is approximately equal to 82.30%.

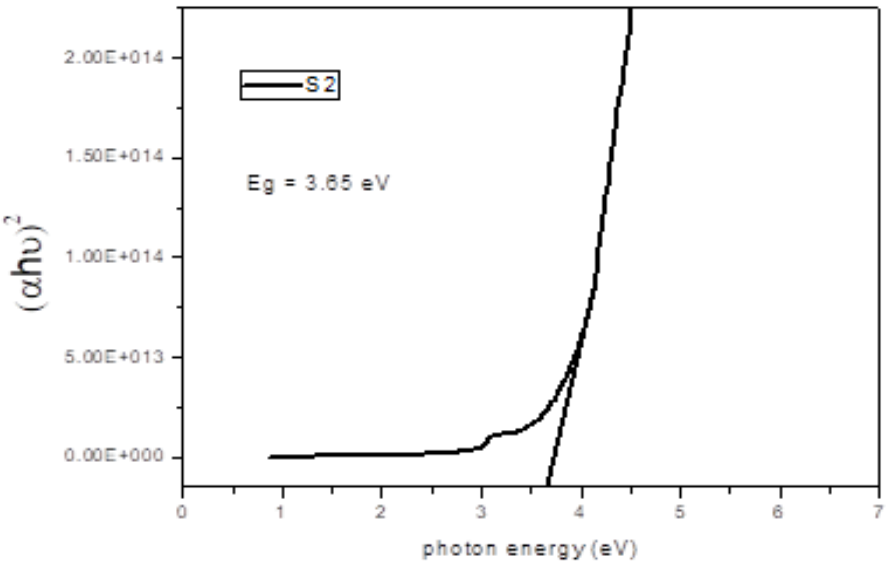

Figure 4.22 Tauc plot of sample S2

From Figure 4.22 energy band gap of sample S2 is 3.65 eV.

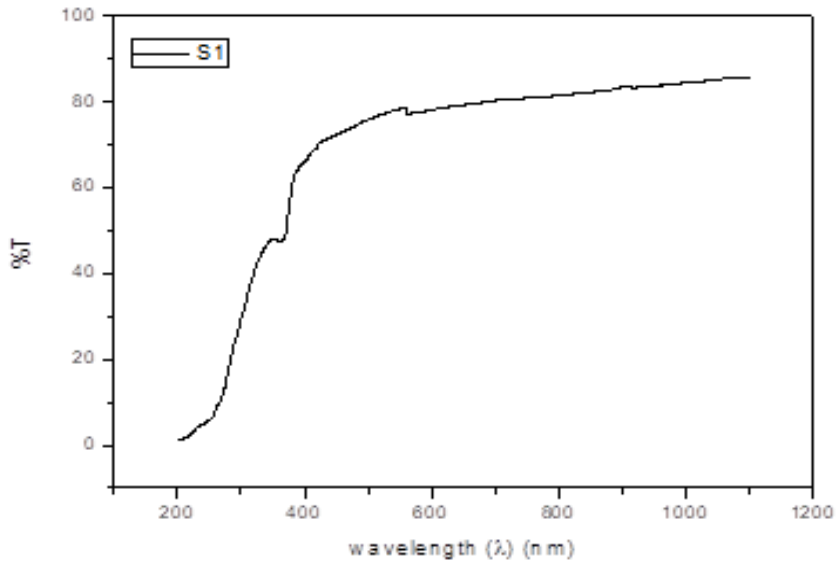

Figure 4.23 UV graph of sample S1

From Figure 4.23 maximum percentage transmittance of sample S1 is approximate 85.74%.

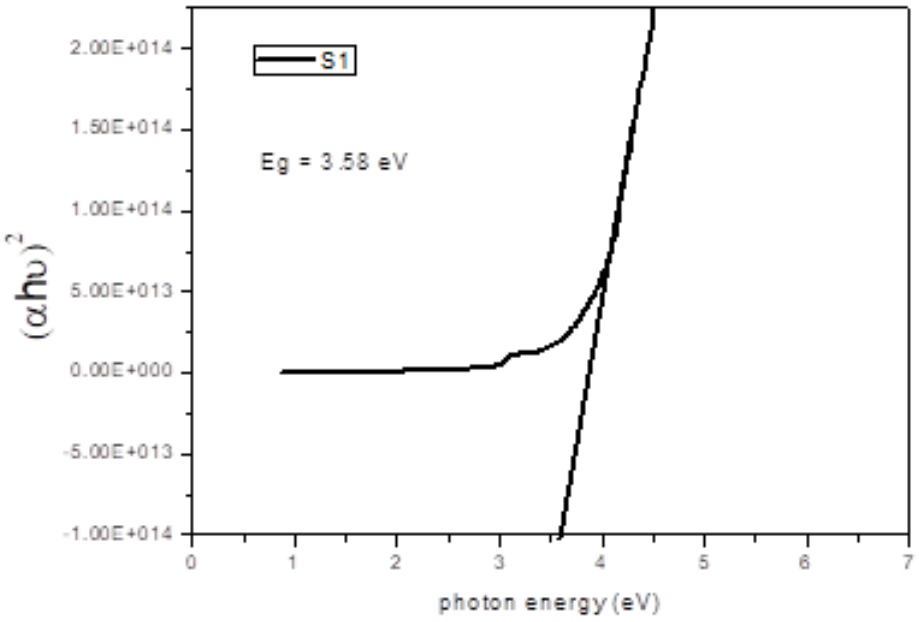

Figure 4.24 Tauc plot of sample S1

From Figure 4.24, sample S1 possess energy band gap of 3.58 eV.

From above study, it can be stated that energy band gap of ZnO thin film decreases as sol molarity increases. From the Tauc plot of sample S1, sample S2, sample S3 Energy band gap becomes approximate equal and ZnO acquire properties of Bulk material. It can be stated from above discussion that conductivity of ZnO increases because energy band gap decreases as sol molarity increases.

4.3 Conclusion

In this chapter we have discussed about xrd results of samples of ZnO thin films. Xrd results shows that a highly crystalline thin film of ZnO has been fabricated or not. From Xrd result we determined average crystallite size.

Further we discussed about gas sensitivity and response time and recovery time of samples. It can be stated that sample S5(0.1M) shows higher sensitivity which is 80% at optimum temperature 300°C among all samples and it shows minimum response time and minimum recovery time which is 23 seconds and 25 seconds among all samples.

From the UV graph and Tauc plot, we determined the energy band gap of all samples. We can say from Tauc plot that as sol molarity increases ZnO thin film acquire bulk material properties because the energy band gap at higher sol molarity becomes approximate equal. It can be stated that conductivity increases of ZnO as energy band gap decreases as sol molarity increases.

Chapter 5

Conclusion and Future scope

5.1 Conclusion

we can conclude that ZnO thin films as sensing layer with various molarity concentration are deposited by the sol gel method using spin coating technique. The surface morphology of the thin films was studied and it was found that surface roughness is increased as average crystallite size (grain size) increases with increasing sol molarity.

The sensitivity results conclude optimum sol molarity to be 0.1M resulting in the highest sensitivity which is 80% towards NOx gas at optimum temperature 300°C.

Further, Energy band gap also varies with variation in sol molarity. The energy band gap decreases with increase in sol molarity and becomes approximate equal when ZnO thin film acquire bulk properties.

5.2 Future Scope

The present work can further be continued with

- Other parametric variations like the thickness optimization for either reducing or oxidizing gases, which will enhance the sensitivity.
- Enhancement of selectivity of gases some dopants/modifiers can be incorporated as catalysts to ZnO thin films.
- Studies related to the surface morphologies of the thin film in order to improve the surface roughness which will contribute to the enhanced sensing responses for the sensor.

References

[1] D. Bagnall, Y. Chen, Z. Zhu, T. Yao, S. Koyama, M. Y. Shen*, et al.*, "Optically pumped lasing of ZnO at room temperature," *Applied Physics Letters,* vol. 70, pp. 2230-2232, 1997.

[2] V. Srikant, V. Sergo, and D. R. Clarke, "Epitaxial Aluminum-Doped Zinc Oxide Thin Films on Sapphire: I, Effect of Substrate Orientation," *Journal of the American Ceramic Society,* vol. 78, pp. 1931-1934, 1995.

[3] G. Carlotti, G. Socino, A. Petri, and E. Verona, "Acoustic investigation of the elastic properties of ZnO films," *Applied Physics Letters,* vol. 51, pp. 1889-1891, 1987.

[4] W. Jeong, S. Kim, and G. Park, "Preparation and characteristic of ZnO thin film with high and low resistivity for an application of solar cell," *Thin Solid Films,* vol. 506, pp. 180-183, 2006.

[5] G. S. Devi, V. B. Subrahmanyam, S. Gadkari, and S. Gupta, "NH3 gas sensing properties of nanocrystalline ZnO based thick films," *Analytica Chimica Acta,* vol. 568, pp. 41-46, 2006.

[6] T. Pauporté and D. Lincot, "Electrodeposition of semiconductors for optoelectronic devices: results on zinc oxide," *Electrochimica Acta,* vol. 45, pp. 3345-3353, 2000.

[7] M. Suchea, S. Christoulakis, K. Moschovis, N. Katsarakis, and G. Kiriakidis, "ZnO transparent thin films for gas sensor applications," *Thin solid films,* vol. 515, pp. 551-554, 2006.

[8] M. Dwivedi, J. Bhargava, A. Sharma, V. Vyas, and G. Eranna, "CO sensor using ZnO thin film derived by RF magnetron sputtering technique," *IEEE Sensors Journal,* vol. 14, pp. 1577-1582, 2014.

[9] H. Gong, J. Hu, J. Wang, C. Ong, and F. Zhu, "Nano-crystalline Cu-doped ZnO thin film gas sensor for CO," *Sensors and Actuators B: Chemical,* vol. 115, pp. 247-251, 2006.

[10] J. Chen, X. Pan, F. Boussaid, A. McKinley, Z. Fan, and A. Bermak, "Breath Level Acetone Discrimination Through Temperature Modulation of a Hierarchical ZnO Gas Sensor," *IEEE Sensors Letters,* vol. 1, pp. 1-4, 2017.

[11] J.-H. Lee, K.-H. Ko, and B.-O. Park, "Electrical and optical properties of ZnO transparent conducting films by the sol–gel method," *Journal of Crystal Growth,* vol. 247, pp. 119-125, 2003.

[12] V. Kumar, N. Singh, R. Mehra, A. Kapoor, L. Purohit, and H. Swart, "Role of film thickness on the properties of ZnO thin films grown by sol-gel method," *Thin Solid Films,* vol. 539, pp. 161-165, 2013.

[13] P. Carcia, R. McLean, M. Reilly, and G. Nunes Jr, "Transparent ZnO thin-film transistor fabricated by rf magnetron sputtering," *Applied Physics Letters,* vol. 82, pp. 1117-1119, 2003.

[14] J. Chen and T. Fujita, "Effects of annealing on photoluminescence of ZnO thin film prepared by vapor phase growth," *Japanese journal of applied physics,* vol. 42, p. 602, 2003.

[15] N. Kakati, S. H. Jee, S. H. Kim, J. Y. Oh, and Y. S. Yoon, "Thickness dependency of sol-gel derived ZnO thin films on gas sensing behaviors," *Thin Solid Films,* vol. 519, pp. 494-498, 2010.

[16] B. Wang, M. Callahan, C. Xu, L. Bouthillette, N. Giles, and D. Bliss, "Hydrothermal growth and characterization of indium-doped-conducting ZnO crystals," *Journal of crystal growth,* vol. 304, pp. 73-79, 2007.

[17] R. Herberholz, M. Igalson, and H. Schock, "Distinction between bulk and interface states in CuInSe 2/CdS/ZnO by space charge spectroscopy," *Journal of Applied Physics,* vol. 83, pp. 318-325, 1998.

[18] S. Trolier-McKinstry and P. Muralt, "Thin film piezoelectrics for MEMS," *Journal of Electroceramics,* vol. 12, pp. 7-17, 2004.

[19] H. Zheng, X. Du, Q. Luo, J. Jia, C. Gu, and Q. Xue, "Wet chemical etching of ZnO film using aqueous acidic salt," *Thin Solid Films,* vol. 515, pp. 3967-3970, 2007.

[20] S. Christoulakis, M. Suchea, M. Katharakis, N. Katsarakis, E. Koudoumas, and G. Kiriakidis, "ZnO Nanostructured transparent thin films by PLD," *Reviews on Advanced Materials Science,* vol. 10, pp. 331-334, 2005.

[21] N. Itagaki, T. Iwasaki, and K. Hoshino, "Substrate for growing wurtzite type crystal and method for manufacturing the same and semiconductor device," ed: Google Patents, 2014.

[22] H. Wu, K. He, D. Qiu, and D. Huang, "Low-temperature epitaxy of ZnO films on Si (0 0 1) and silica by reactive e-beam evaporation," *Journal of Crystal Growth,* vol. 217, pp. 131-137, 2000.

[23] C. Jagadish and S. J. Pearton, *Zinc oxide bulk, thin films and nanostructures: processing, properties, and applications*: Elsevier, 2011.

[24] C. S. Kumar, *UV-VIS and photoluminescence spectroscopy for nanomaterials characterization*: Springer, 2013.

[25] Y. Ryu, T.-S. Lee, J. A. Lubguban, H. W. White, B.-J. Kim, Y.-S. Park*, et al.*, "Next generation of oxide photonic devices: ZnO-based ultraviolet light emitting diodes," *Applied Physics Letters,* vol. 88, p. 241108, 2006.

[26] L. Stolt, J. Hedström, J. Kessler, M. Ruckh, K. O. Velthaus, and H. W. Schock, "ZnO/CdS/CuInSe2 thin-film solar cells with improved performance," *Applied Physics Letters,* vol. 62, pp. 597-599, 1993.

[27] M. Dutta, S. Mridha, and D. Basak, "Effect of sol concentration on the properties of ZnO thin films prepared by sol–gel technique," *Applied Surface Science,* vol. 254, pp. 2743-2747, 2008.

[28] S. M. Sze, *Semiconductor devices: physics and technology*: John Wiley & Sons, 2008.

[29] A. Hashim, M. Jaafar, A. J. Ghazai, and N. Ahmed, "Fabrication and characterization of ZnO thin film using sol–gel method," *Optik-International Journal for Light and Electron Optics,* vol. 124, pp. 491-492, 2013.

[30] A. Paliwal, A. Sharma, M. Tomar, and V. Gupta, "Dielectric dispersion of rf Sputter-deposited SnO 2, ZnO, WO 3 thin films using surface plasmon resonance technique," *IEEE Transactions on Dielectrics and Electrical Insulation,* vol. 22, pp. 3529-3535, 2015.

[31] B. Jin, S. Im, and S. Y. Lee, "Violet and UV luminescence emitted from ZnO thin films grown on sapphire by pulsed laser deposition," *Thin Solid Films,* vol. 366, pp. 107-110, 2000.

[32] H. Morkoç and Ü. Özgür, *Zinc oxide: fundamentals, materials and device technology*: John Wiley & Sons, 2008.

[33] L. Znaidi, T. Chauveau, A. Tallaire, F. Liu, M. Rahmani, V. Bockelee*, et al.*, "Textured ZnO thin films by sol–gel process: Synthesis and characterizations," *Thin Solid Films,* vol. 617, pp. 156-160, 2016.

[34] J. Guo, J. Zhang, M. Zhu, D. Ju, H. Xu, and B. Cao, "High-performance gas sensor based on ZnO nanowires functionalized by Au nanoparticles," *Sensors and Actuators B: Chemical,* vol. 199, pp. 339-345, 2014.

[35] R. Pawar, J. Shaikh, A. Moholkar, S. Pawar, J. Kim, J. Patil*, et al.*, "Surfactant assisted low temperature synthesis of nanocrystalline ZnO and its gas sensing properties," *Sensors and Actuators B: Chemical,* vol. 151, pp. 212-218, 2010.

[36] M. Deshwal and A. Arora, "Enhanced acetone detection using Au doped ZnO thin film sensor," *Journal of Materials Science: Materials in Electronics,* pp. 1-6, 2018.

[37] B. D. Cullity and S. R. Stock, *Elements of X-ray Diffraction*: Pearson Education, 2014.

[38] R. Jenkins and R. L. Snyder, *Introduction to X-ray Powder Diffractometry (Volume 138)*: Wiley Online Library, 1996.

[39] M. Birkholz, *Thin film analysis by X-ray scattering*: John Wiley & Sons, 2006.

[40] F. Scholz, *Compound Semiconductors: Physics, Technology, and Device Concepts*: Pan Stanford, 2017.

[41] D. Dorset, "X-ray diffraction: a practical approach," *Microscopy and microanalysis,* vol. 4, pp. 513-515, 1998.

[42] O. Stenzel, *The physics of thin film optical spectra*: Springer, 2005.

[43] A. Sharma, M. Tomar, and V. Gupta, "WO3 nanoclusters–SnO2 film gas sensor heterostructure with enhanced response for NO2," *Sensors and Actuators B: Chemical,* vol. 176, pp. 675-684, 2013.

[44] D. Haridas, A. Chowdhuri, K. Sreenivas, and V. Gupta, "Effect of thickness of platinum catalyst clusters on response of SnO2 thin film sensor for LPG," *Sensors and Actuators B: Chemical,* vol. 153, pp. 89-95, 2011.

[45] H. Bian, S. Ma, A. Sun, X. Xu, G. Yang, S. Yan*, et al.*, "Improvement of acetone gas sensing performance of ZnO nanoparticles," *Journal of Alloys and Compounds,* vol. 658, pp. 629-635, 2016.

[46] M. Kumar, A. Kumar, and A. Abhyankar, "SnO2 based sensors with improved sensitivity and response-recovery time," *Ceramics International,* vol. 40, pp. 8411-8418, 2014.

List of Publications

Communicated

A. Kumar Bhatt, M.Deshwal, A. Arora, “Effect of variation in Sol-Molarity on crystallite size of ZnO thin film for gas sensing application” Material performance.

Status: Under review